Modelling microstructure of irradiated tungsten: from micro- to meso-scales

S.L. Dudarev[1,2], A.E. Sand[3], D. Mason[1], X. Yi[1,2], M.A. Kirk[4], F. Hoffman[5], D. Nguyen-Manh[1], K. Nordlund[3]

[1]CCFE, UK Atomic Energy Authority, Oxfordshire, UK.
[2]Department of Materials, University of Oxford, Oxford, UK.
[3]Department of Physics, University of Helsinki, Finland.
[4]Materials Science Division, Argonne National Laboratory, USA.
[5]Department of Engineering, University of Oxford, Oxford, UK.

Outline

- Integration of neutron transport and materials simulations.
- Production of radiation damage: defect cluster size scaling laws.
- Evolution of damage at elevated temperatures.
- Formation of ordered defect structures.
- Helium-induced swelling in tungsten, defect relaxation volumes.

ILW – Before campaign

ILW – After campaign

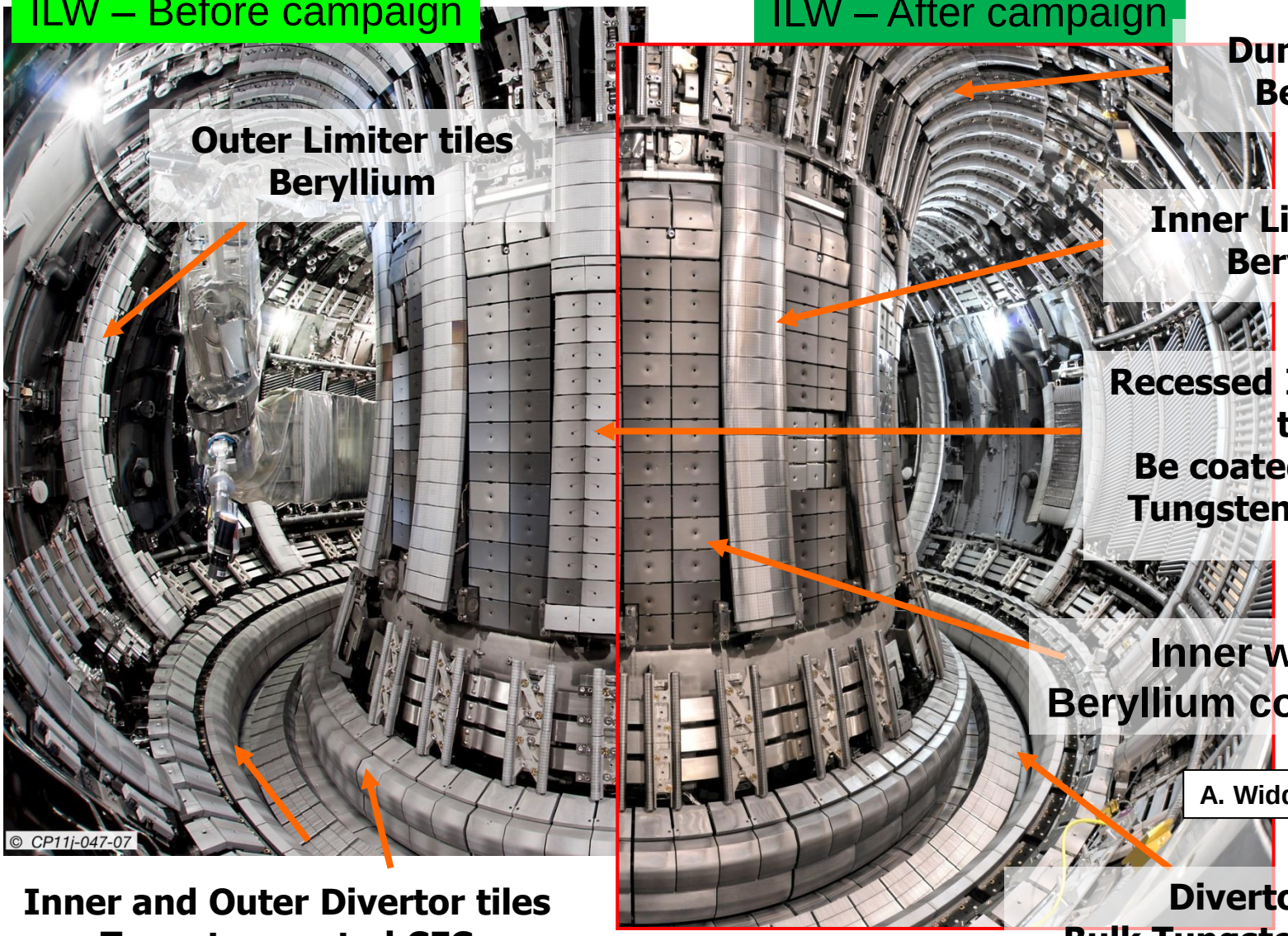

United Kingdom Atomic Energy Authority

ITER-Like Wall (ILW) at JET

CCFE is the fusion research arm of the **United Kingdom Atomic Energy Authority**

CCFE CULHAM CENTRE FOR FUSION ENERGY

IOP Publishing and International Atomic Energy Agency
Nucl. Fusion 52 (2012) 083019 (12pp)
Nuclear Fusion
doi:10.1088/0029-5515/52/8/083019

An integrated model for materials in a fusion power plant: transmutation, gas production, and helium embrittlement under neutron irradiation

M.R. Gilbert, S.L. Dudarev, S. Zheng, L.W. Packer and J.-Ch. Sublet

EURATOM/CCFE Fusion Association, Culham Centre for Fusion Energy, Abingdon, Oxfordshire OX14 3DB, UK

E-mail: mark.gilbert@ccfe.ac.uk

Received 16 January 2012, accepted for publication 11 July 2012
Published 1 August 2012
Online at stacks.iop.org/NF/52/083019

Abstract

The high-energy, high-intensity neutron fluxes produced by the fusion plasma will have a significant life-limiting impact on reactor components in both experimental and commercial fusion devices. As well as producing defects, the neutrons bombarding the materials initiate nuclear reactions, leading to transmutation of the elemental atoms. Products of many of these reactions are gases, particularly helium, which can cause swelling and embrittlement of materials.

This paper integrates several different computational techniques to produce a comprehensive picture of the response of materials to neutron irradiation, enabling the assessment of structural integrity of components in a fusion power plant. Neutron-transport calculations for a model of the next-step fusion device DEMO reveal the variation in exposure conditions in different components of the vessel, while inventory calculations quantify the associated implications for transmutation and gas production. The helium production rates are then used, in conjunction with a simple model for He-induced grain-boundary embrittlement based on electronic-structure density functional theory calculations, to estimate the timescales for susceptibility to grain-boundary failure in different fusion-relevant materials. There is wide variation in the predicted grain-boundary-failure lifetimes as a function of both microstructure and chemical composition, with some conservative predictions indicating much less than the required lifetime for components in a fusion power plant.

(Some figures may appear in colour only in the online journal)

1. Introduction

In magnetic-confinement fusion devices a large number of high-energy neutrons are generated in the plasma by deuterium–tritium fusion reactions. These neutrons escape from the plasma and irradiate the materials that make up the reactor vessel. One of the key outstanding issues for the fusion materials programme is in the understanding of how neutrons influence the properties of materials over the projected lifetime of a fusion power plant. Not only do the incident neutrons cause atomic displacements within the materials, leading to the generation and accumulation of radiation defects, which cause hardening, embrittlement, and irradiation creep, but they also initiate non-elastic nuclear reactions that alter the nature of the constituent atoms. This process, known as transmutation or burn-up, changes the chemical composition of materials, leading in turn to measurable changes in structural and mechanical properties.

Perhaps even more problematic are the nuclear reactions initiated by fusion neutrons that give rise to the transmutation production of gas atoms, such as helium (He) and hydrogen (H). These reactions, which include neutron capture followed by α-particle ($^4He^{2+}$) emission, often written as (n,α), and neutron capture and proton ($^1H^+$) emission (n,p), generally occur less frequently than the major (n,γ) reactions, but have a much more significant effect on properties of materials, particularly metals and alloys. Even at low concentrations, gas particles can have severe life-limiting consequences for materials, with He being a particular problem because, with its low solubility in the crystal lattice, it forms clusters and accumulates at defects, dislocations and at grain boundaries, leading to swelling or embrittlement.

In fusion, the issue of transmutation gas production is likely to be a more significant problem than in fission because of the higher neutron fluxes and higher average neutron energies. For example, in figure 1 where a fission spectrum

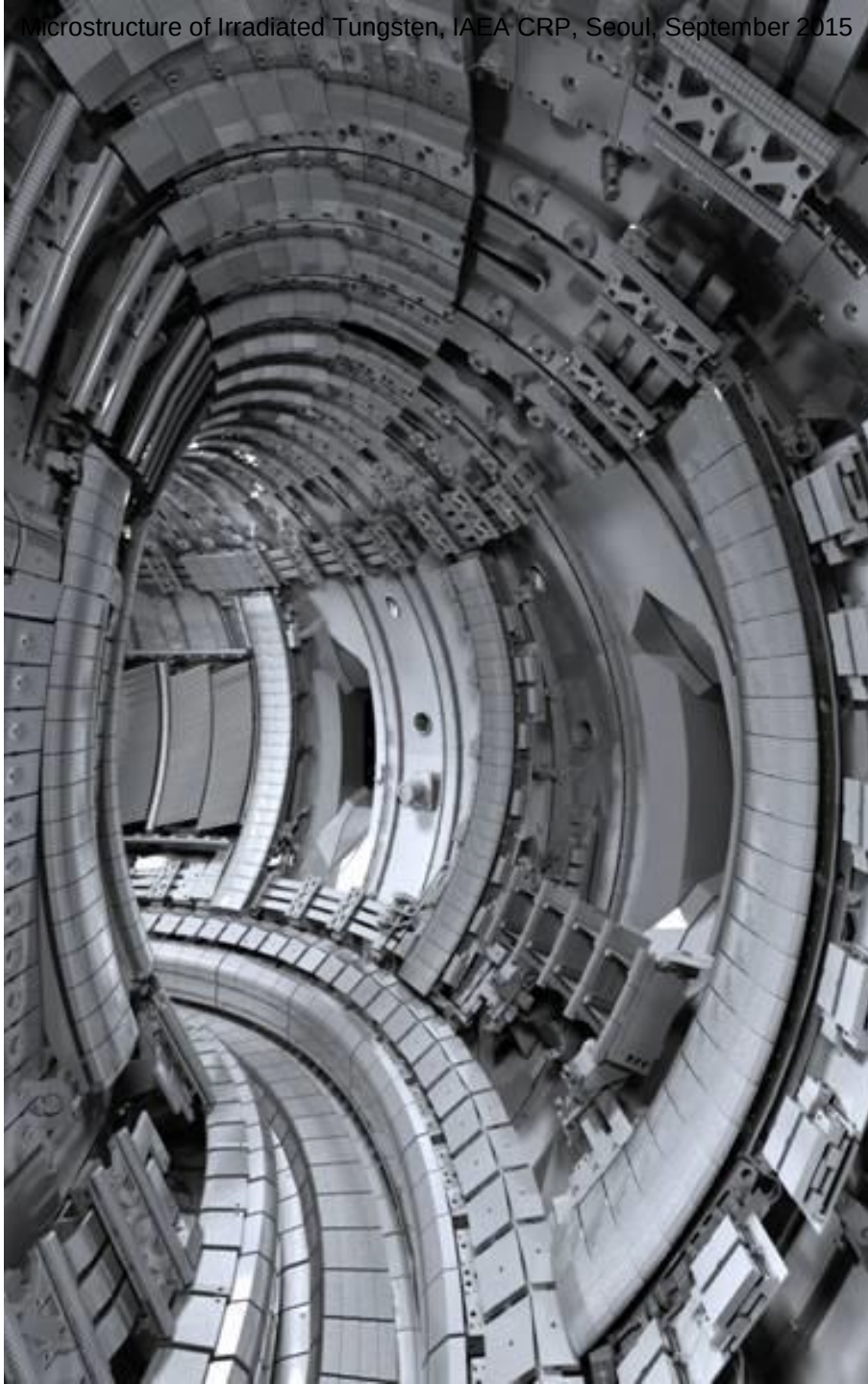

Integrated materials lifetime assessment

Plasma as a 3D neutron source

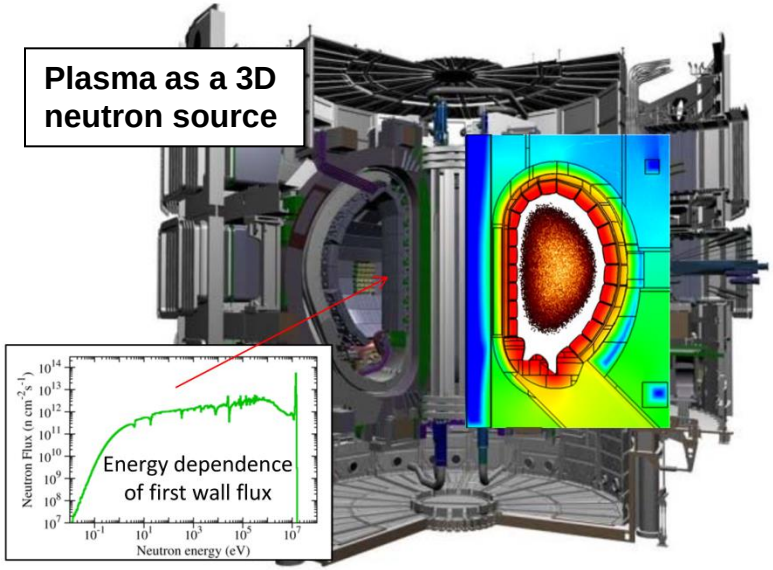

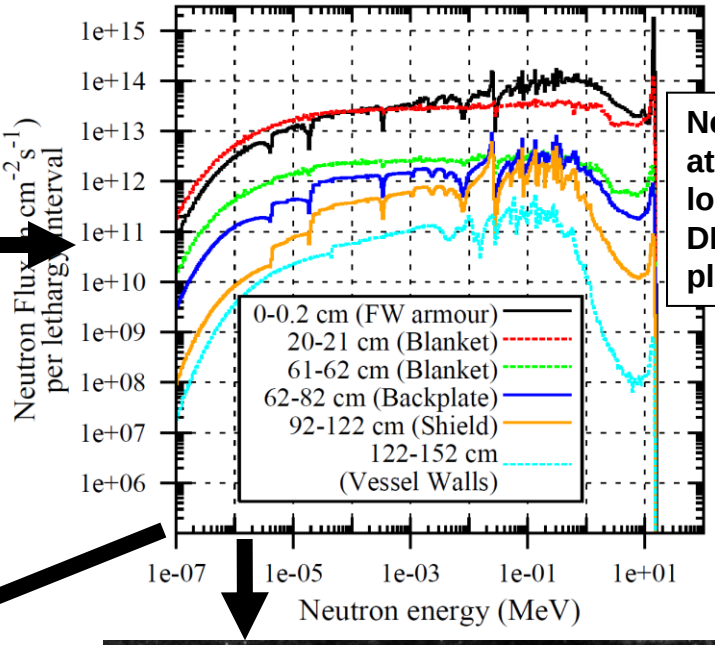

Neutron spectra at various locations in a DEMO power plant

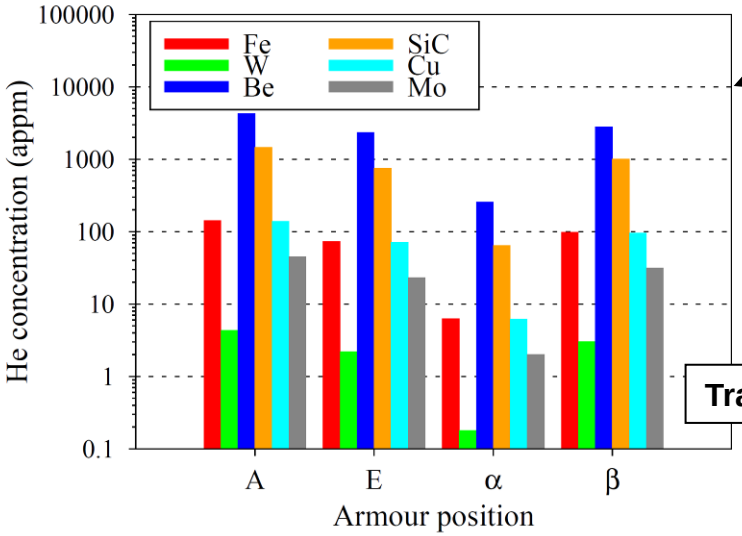

Transmutations

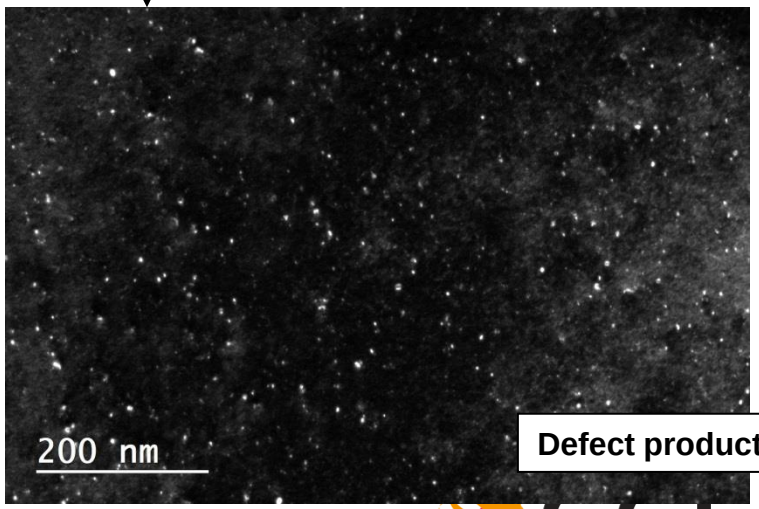

Defect production

M.R. Gilbert *et al*., Nucl. Fusion 52 (2012) 083019; J. Nucl. Mater. 442 (2013) S755

Radiation damage effects in tungsten

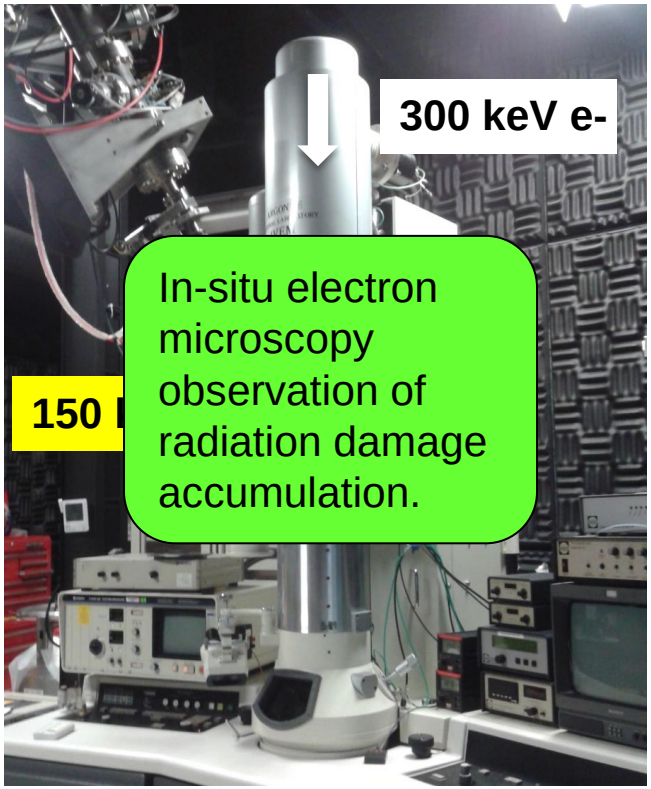

In-situ electron microscopy observation of radiation damage accumulation.

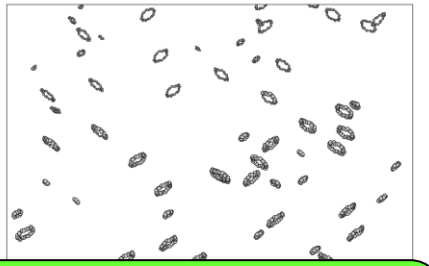

Ordering of radiation defects in irradiated tungsten.

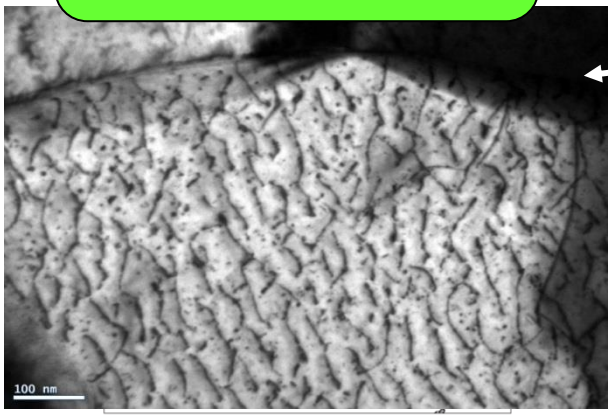

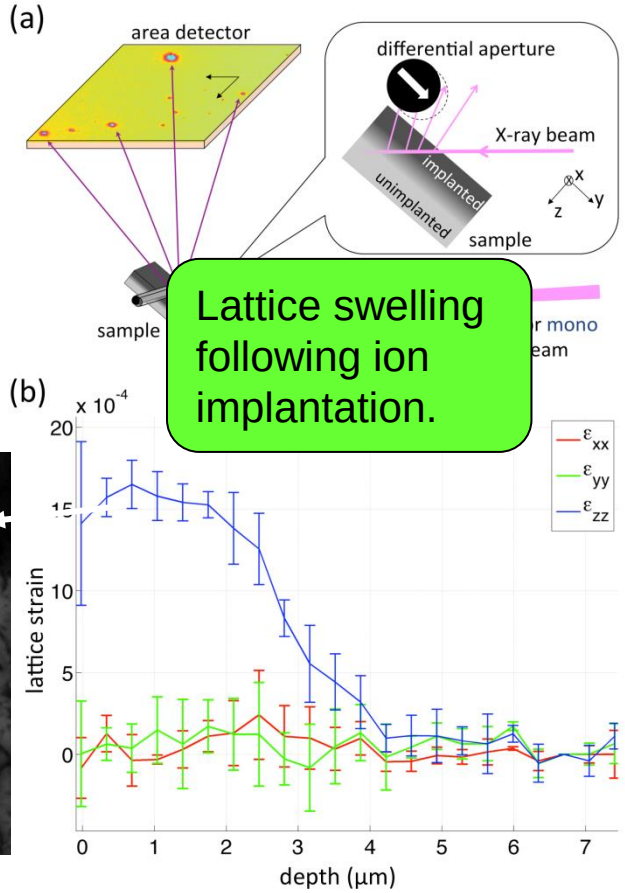

Lattice swelling following ion implantation.

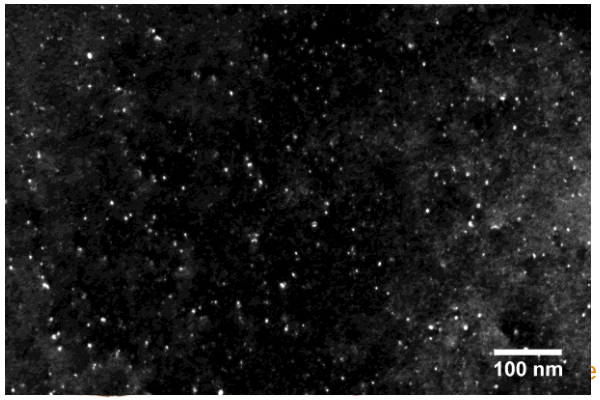

Left: X. Yi, A.E. Sand, D.R. Mason, M.A. Kirk, S.G. Roberts, K. Nordlund, and S.L. Dudarev, EuroPhysics Letters (EPL) **110** (2015) 36001

Centre: S.L. Dudarev, K. Arakawa, X. Yi, Z. Yao, M.L. Jenkins, M.R. Gilbert, P.M. Derlet, Journal of Nuclear Materials 455 (2014) 16–20

Right: F. Hofmann, D. Nguyen-Manh, M.R. Gilbert, C.E. Beck, J.K. Eliason, A.A. Maznev, W. Liu, D.E.J. Armstrong, K.A. Nelson, and S.L. Dudarev, Acta Materialia **89** (2015) 352–363

CENTRE FOR FUSION ENERGY

Defect production in cascades

Defect production in tungsten

The maximum cascade energy is (a non-relativistic equation assuming head-on elastic neutron-atom impact)

$$E_{\max} \approx \frac{4mM}{(m+M)^2} E_n \approx 300\ \text{keV};$$

$$E_n = 14.1\ \text{MeV}$$

A 150 keV cascade in tungsten: a high energy "fusion" cascade

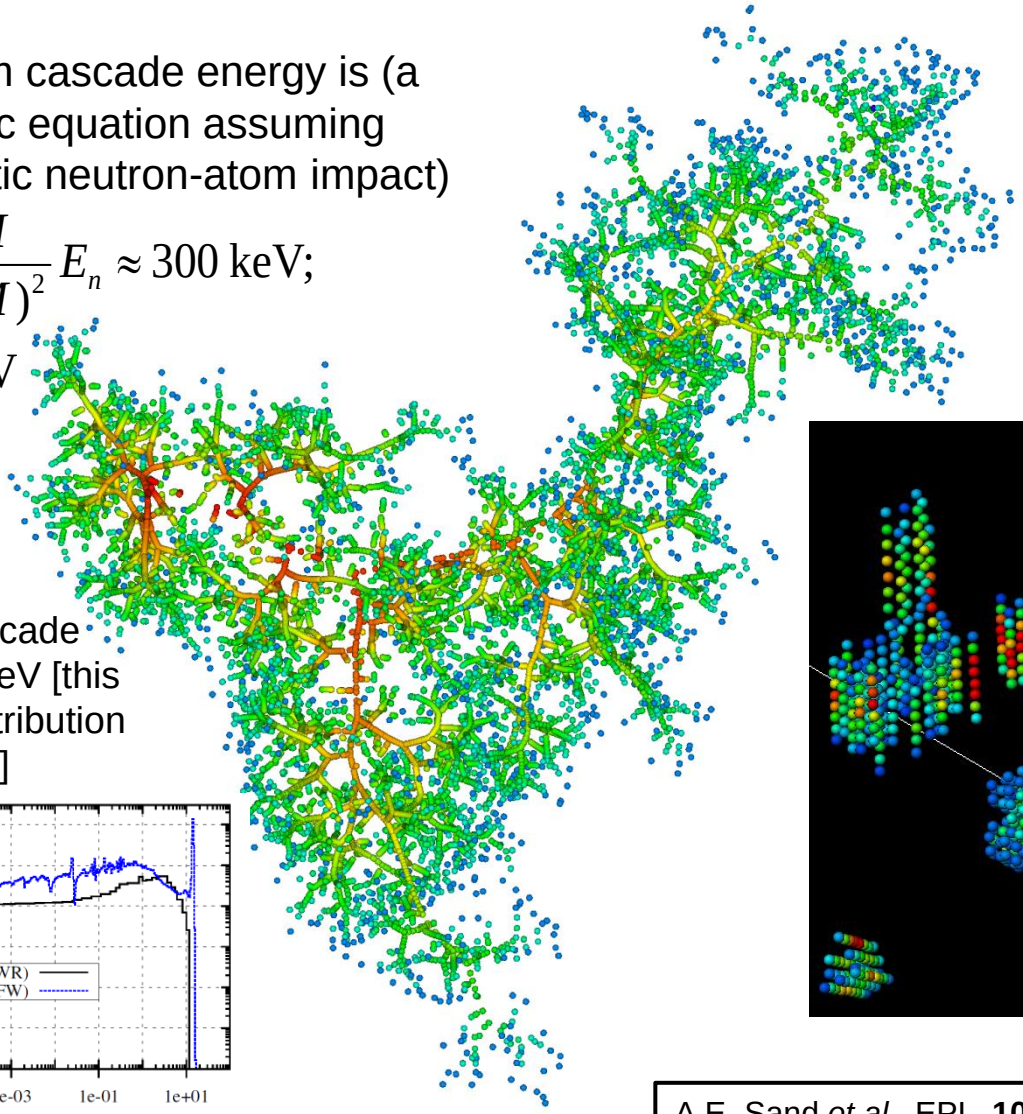

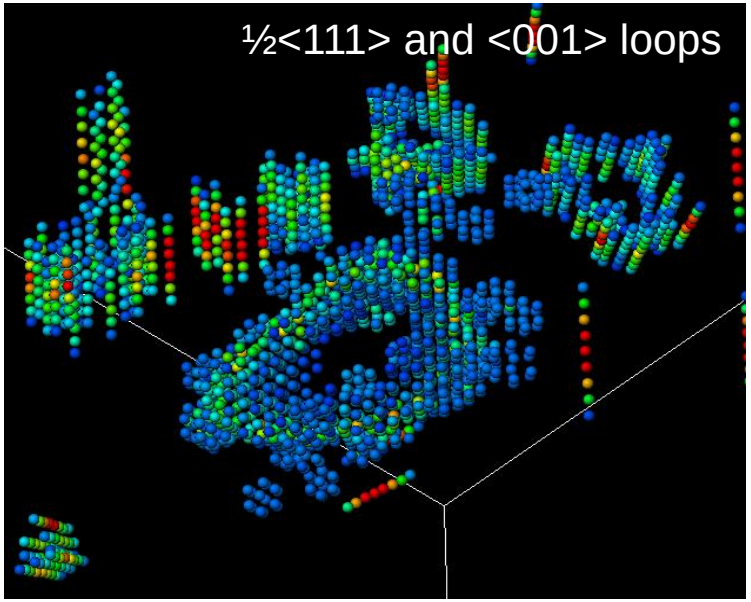

The average cascade energy is ~150 keV [this neglects the contribution of (n,γ) reactions]

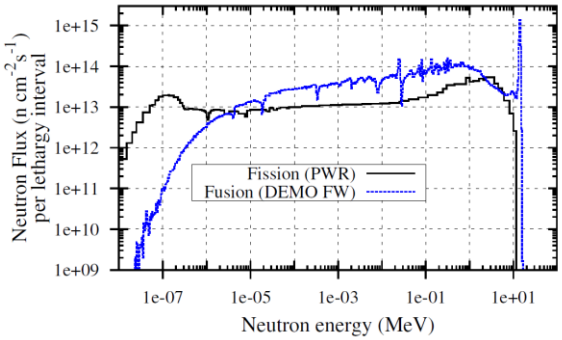

A.E. Sand *et al.*, EPL **103** (2013) 46003

Defect production in tungsten

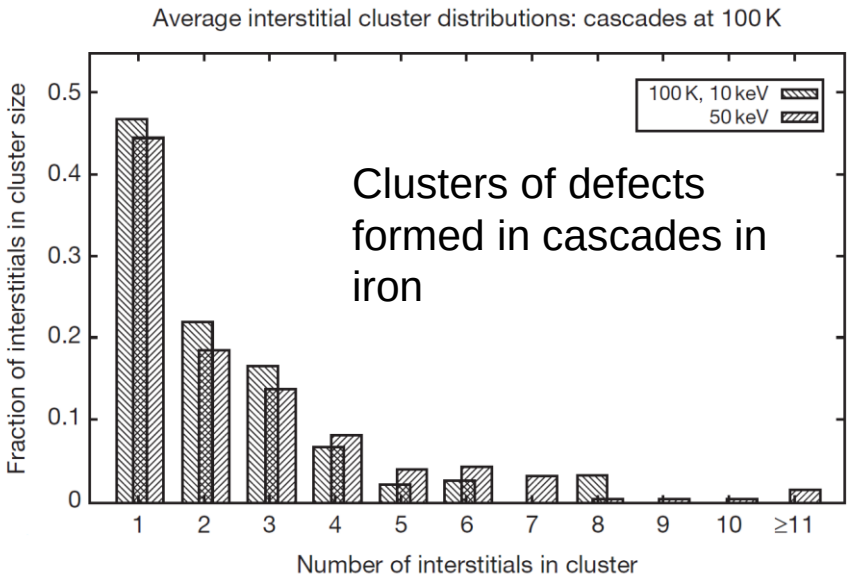

R.E. Stoller (2012) in: Comprehensive Nuclear Materials

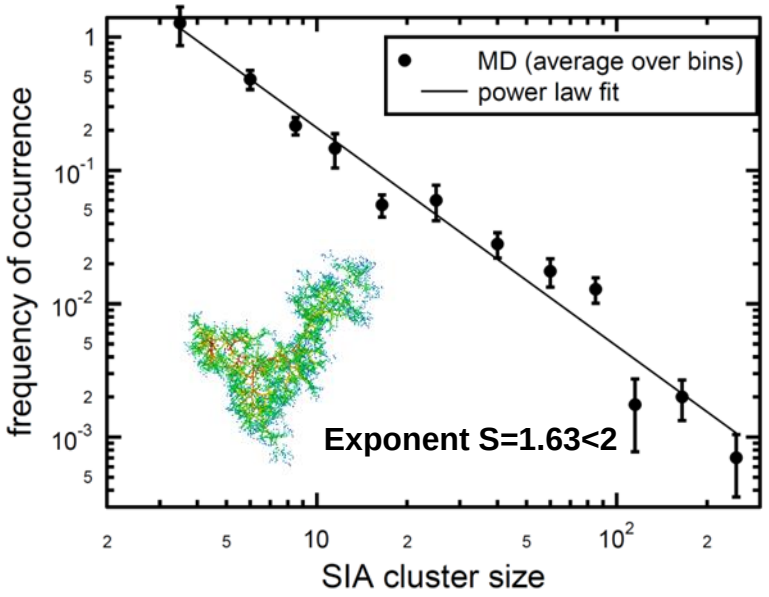

Prior to 1991 it was assumed that defects were produced as Frenkel pairs (individual vacancies and self-interstitials). C.H. Woo and B.N. Singh (1991) noted that clustering of defects in cascades may have a significant effect on radiation-induced microstructure.

T. Diaz de la Rubia, M.W. Guinan, PRL **66** (1991) 2766;
C.H. Woo, B.N. Singh, Phil. Mag. **65** (1992) 889-912

Distribution of defect cluster sizes follows a power law

$$F(n) = \frac{A}{n^S}; n < n^* \approx 600$$

$$A \approx 7.45; S = 1.63 < 2$$

A.E. Sand *et al.*, EPL **103** (2013) 46003

The power law of defect size distribution

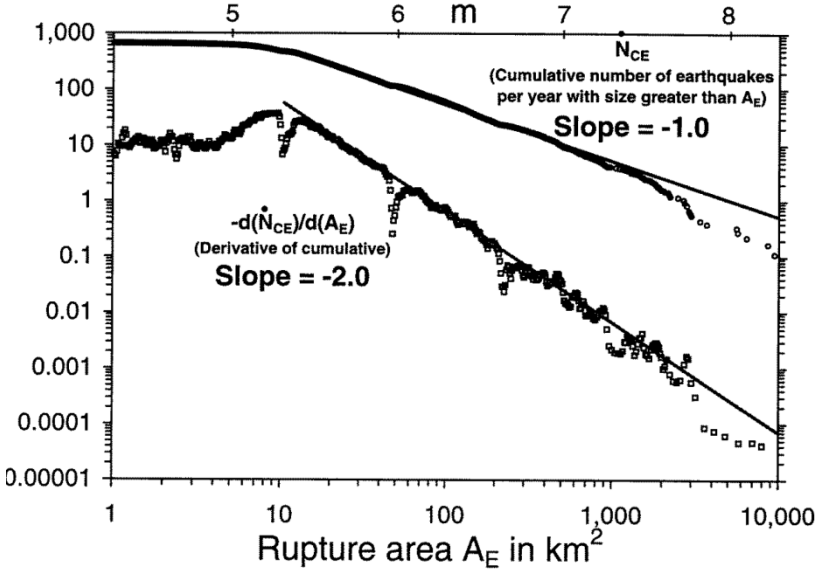

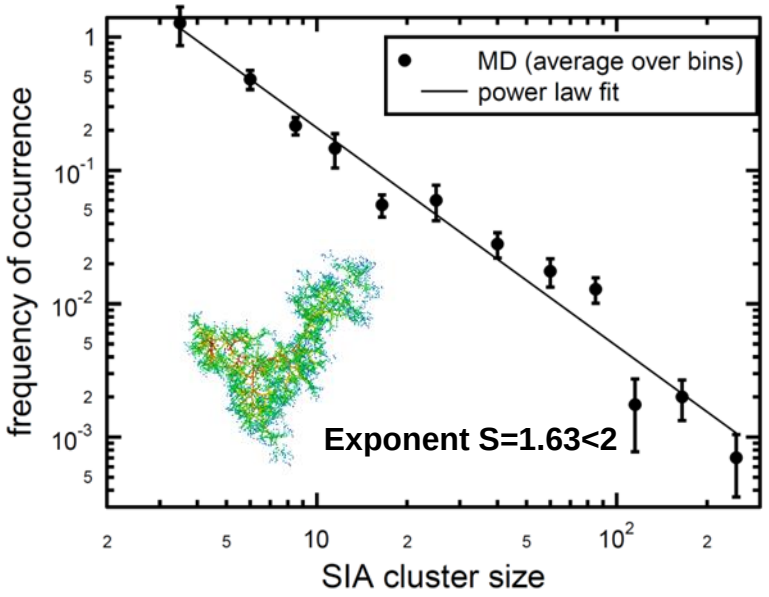

Total number of defects produced

$$N = \int_1^{n^*} nF(n)dn \approx \frac{A}{2-S}(n^*)^{2-S}$$

Large clusters are rare BUT once they form they contain the majority of defects. Large rarely occurring defects dominate microstructural evolution.

Distribution of defect cluster sizes follows a power law

$$F(n) = \frac{A}{n^S}; n < n^* \approx 600$$

$$A \approx 7.45; S = 1.63 < 2$$

A.E. Sand *et al.*, EPL **103** (2013) 46003

A Letters Journal Exploring the Frontiers of Physics

May 2015

EPL, **110** (2015) 36001
doi: 10.1209/0295-5075/110/36001

www.epljournal.org

Direct observation of size scaling and elastic interaction between nano-scale defects in collision cascades

X. Yi[1,2], A. E. Sand[3], D. R. Mason[2], M. A. Kirk[4], S. G. Roberts[1,2], K. Nordlund[3] and S. L. Dudarev[2,1]

[1] *Department of Materials, University of Oxford - Parks Road, Oxford, OX1 3PH, UK*
[2] *CCFE, Culham Centre for Fusion Energy - Abingdon, Oxfordshire OX14 3DB, UK*
[3] *Department of Physics, University of Helsinki - P. O. Box 43, FI-00014, Helsinki, Finland*
[4] *Nuclear Engineering Division, Argonne National Laboratory - Argonne, IL 60439, USA*

received 2 March 2015; accepted in final form 24 April 2015
published online 14 May 2015

PACS 61.72.J- – Point defects and defect clusters
PACS 61.80.Az – Theory and models of radiation effects
PACS 68.37.Lp – Transmission electron microscopy (TEM)

Abstract – Using *in situ* transmission electron microscopy, we have directly observed nano-scale defects formed in ultra-high–purity tungsten by low-dose high-energy self-ion irradiation at 30 K. At cryogenic temperature lattice defects have reduced mobility, so these microscope observations offer a window on the initial, primary damage caused by individual collision cascade events. Electron microscope images provide direct evidence for a power-law size distribution of nano-scale defects formed in high-energy cascades, with an upper size limit independent of the incident ion energy, as predicted by Sand *et al.* (*EPL*, **103** (2013) 46003). Furthermore, the analysis of pair distribution functions of defects observed in the micrographs shows significant intra-cascade spatial correlations consistent with strong elastic interaction between the defects.

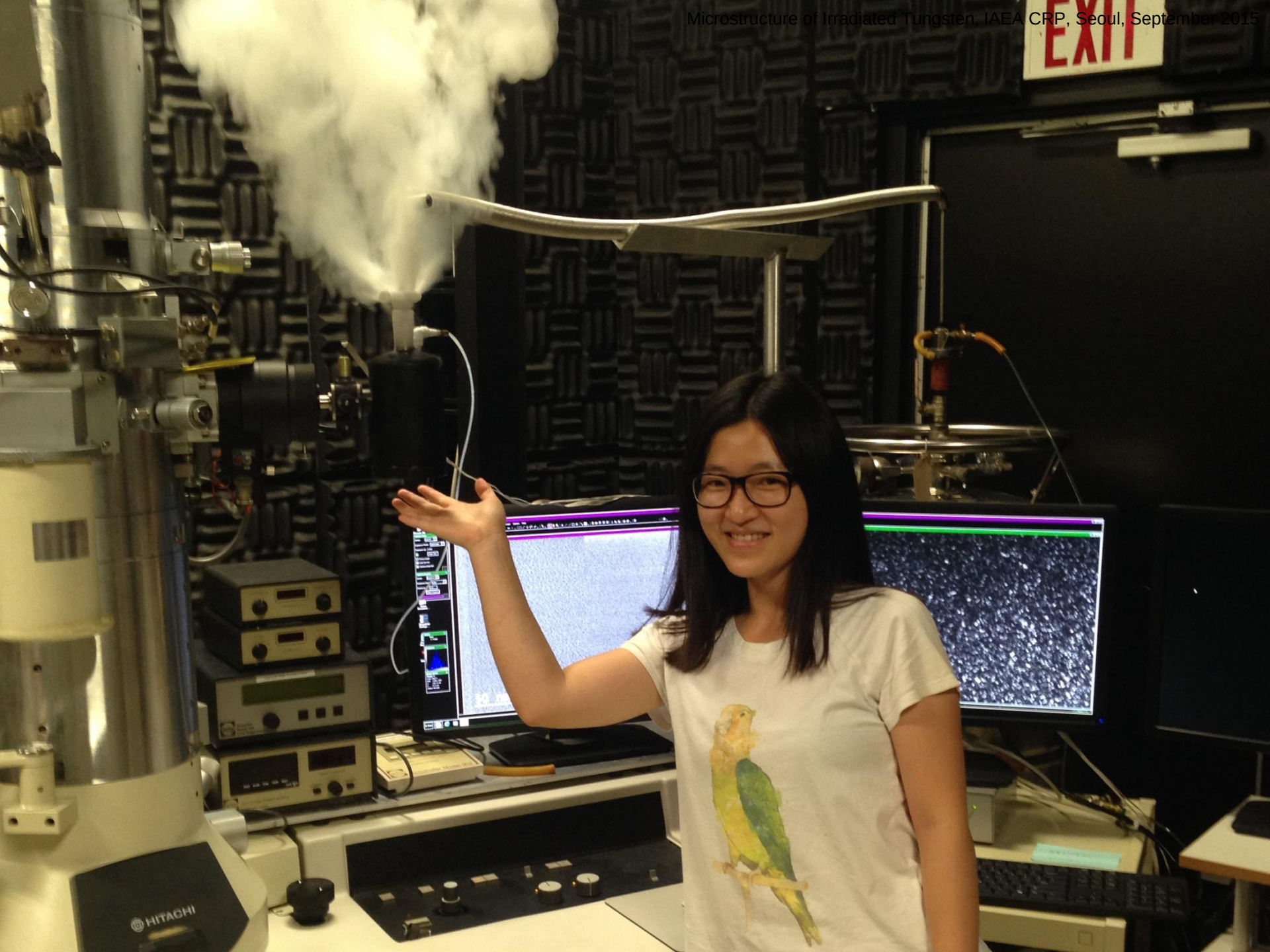
EXIT
HITACHI

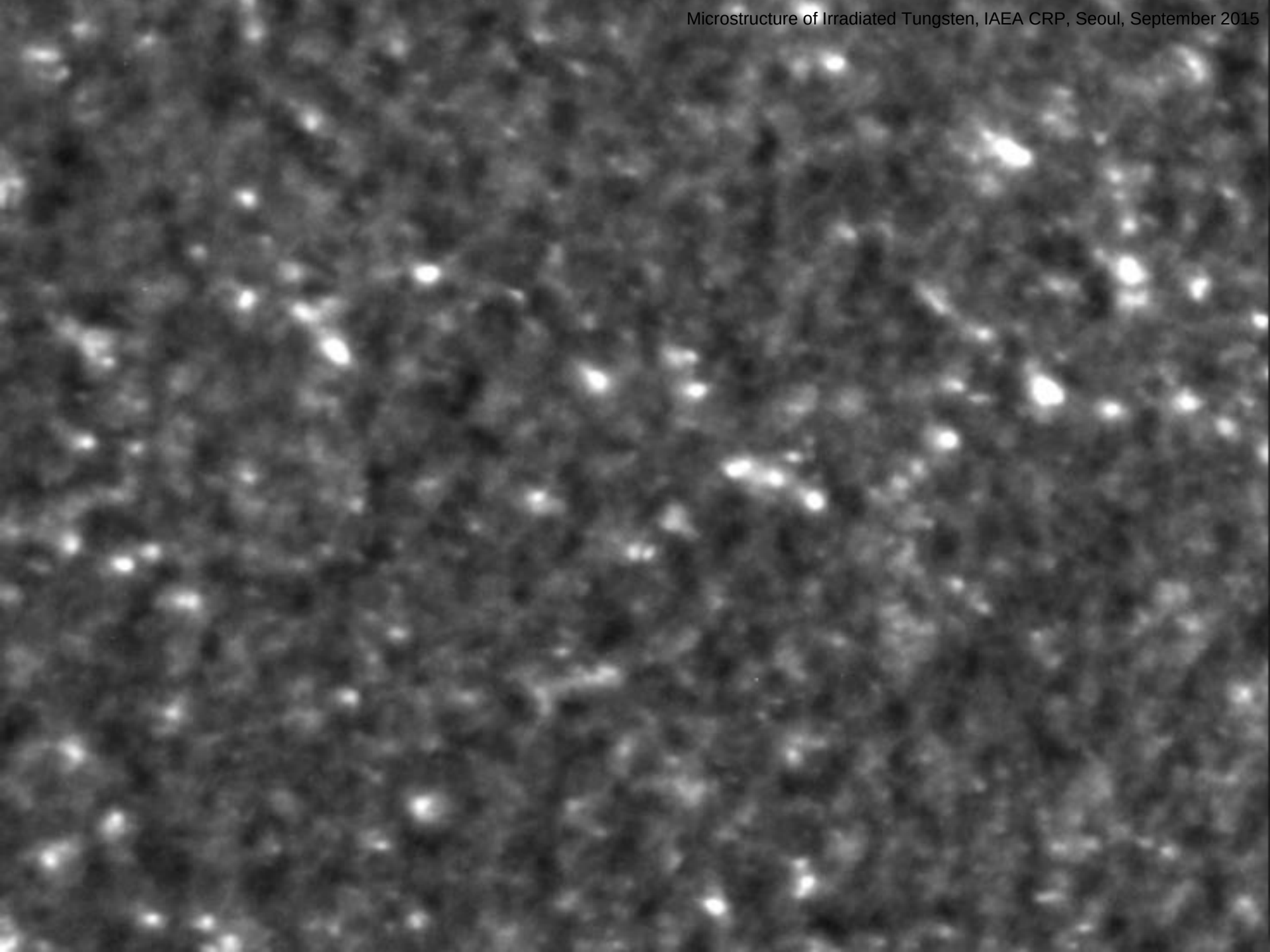

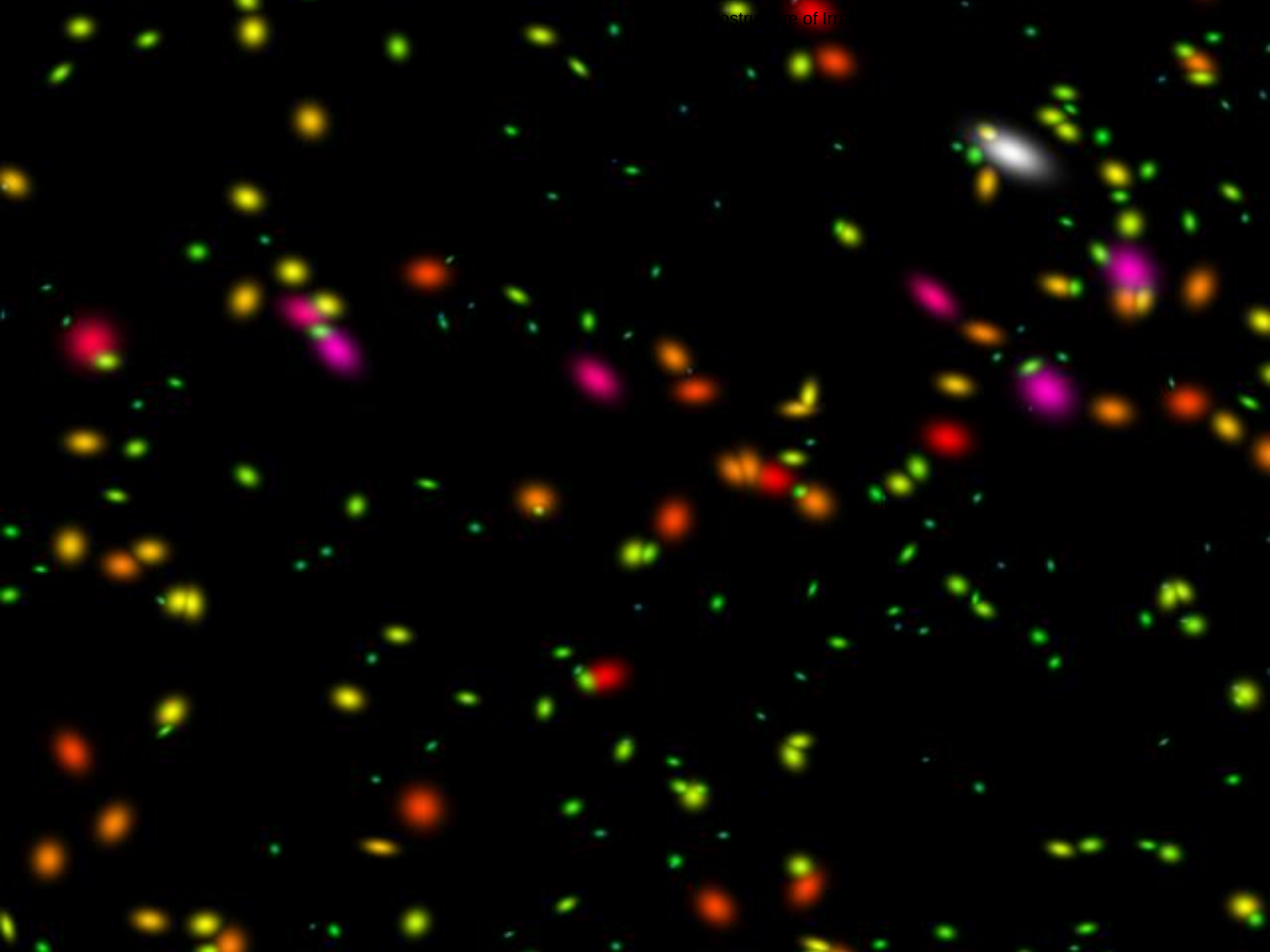

Defect size scaling: experimental validation

Electron microscope images provide data on defect sizes

A scaling law for radiation defect sizes discovered earlier (2013) in MD simulations of collision cascades in tungsten, has now been confirmed and extended to a much broader range of sizes using direct electron microscope observations – a critical step in quantifying radiation effects in materials.

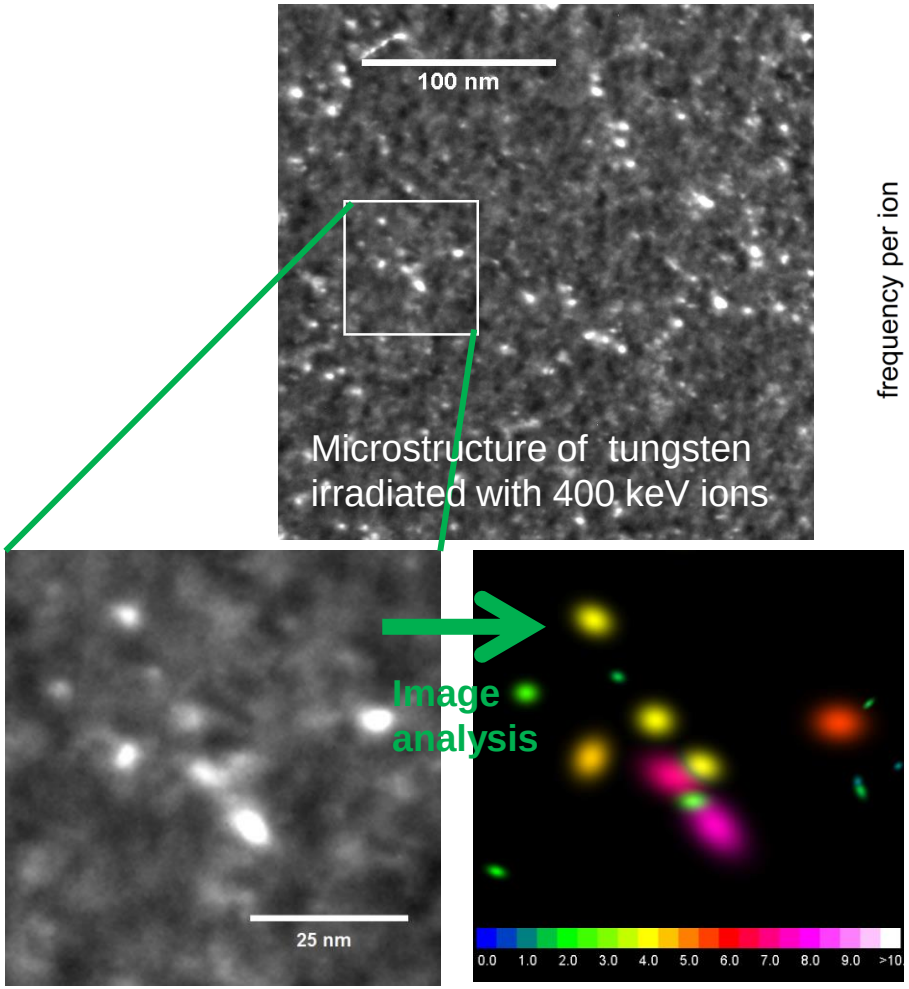

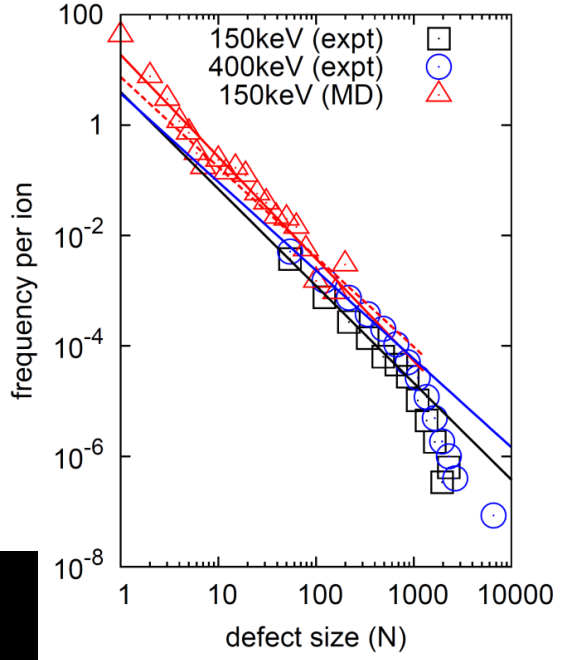

$$F(n) = \frac{A}{n^S}; n < n^* \approx 600$$

$$A \approx 2.7\,; S \approx 1.8 < 2$$

United Kingdom Atomic Energy Authority

X. Yi, A.E. Sand, D.R. Mason *et al.* EPL 110 (2015) 36001

CCFE CULHAM CENTRE FOR FUSION ENERGY

Evolution of defects produced in cascades

Experimental observations: temperature effects

Defects in pure W, 1 dpa in (001)-grains

X. Yi, M.L. Jenkins, M.A. Kirk (2012)

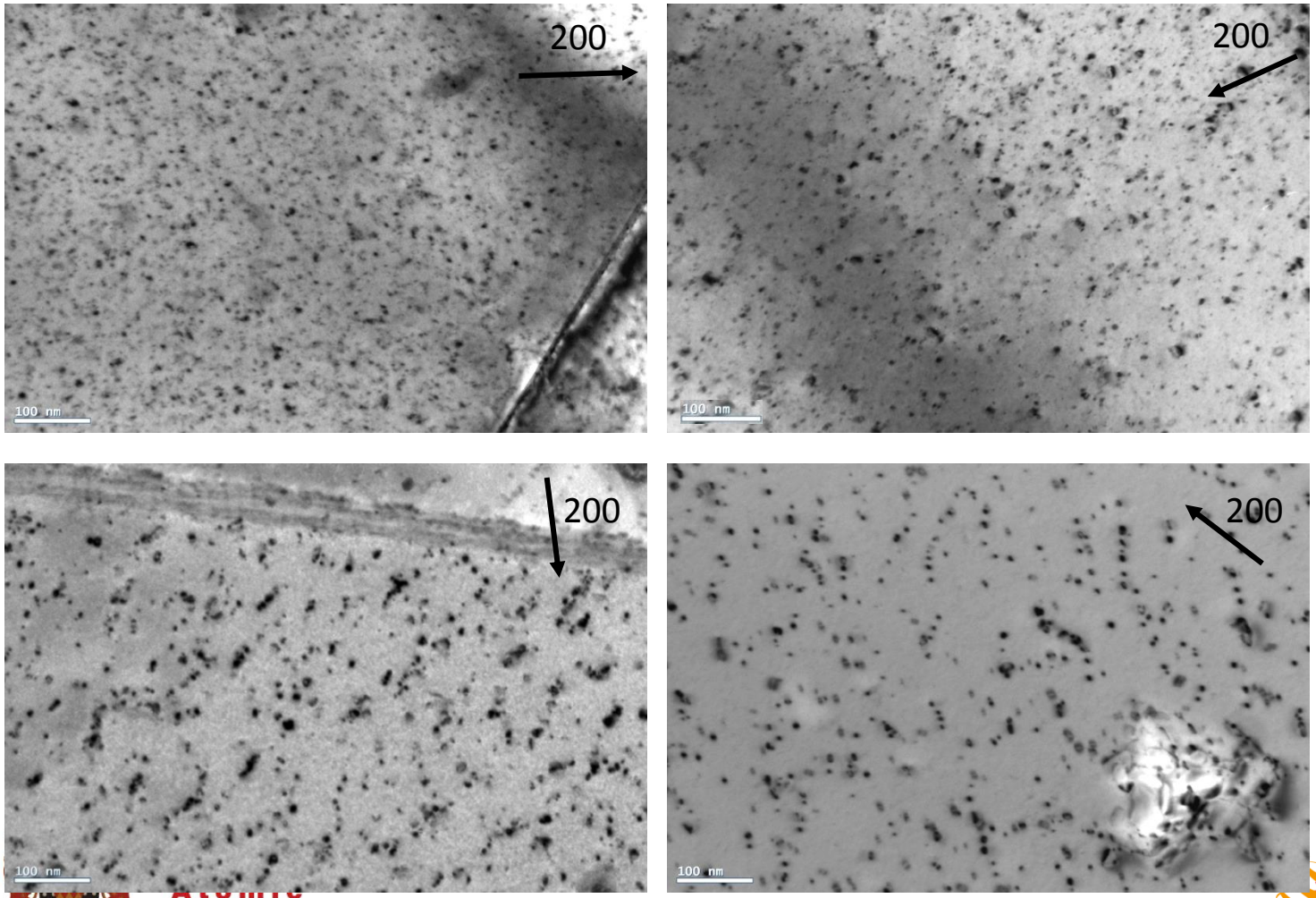

300° C	500° C
600° C	800° C

Defects observed at elevated temperatures have larger size.

They also form ordered structures.

Direct observation of accumulation of radiation defects

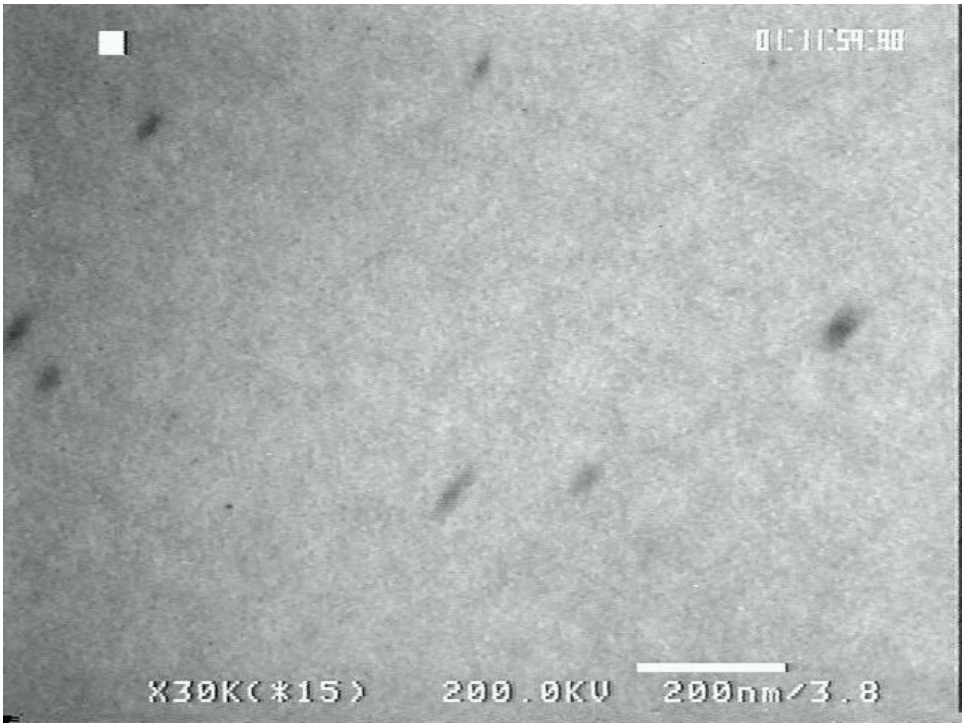

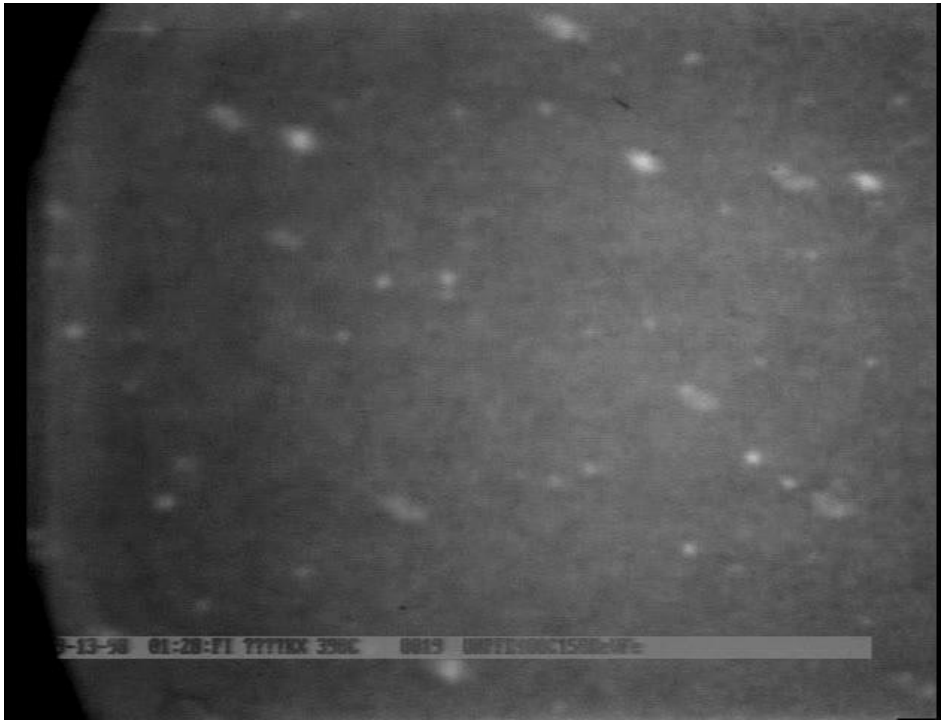

In-situ electron microscope observation of accumulation of radiation defects under self-ion irradiation. Left: Brownian motion of glissile 111 prismatic dislocation loops in Fe at 675K [courtesy of Prof. K. Arakawa, Shimane Uni. Japan]. Right: self-ion irradiation of ultra-high purity iron at 400°C, viewed at x30 real time [courtesy of Prof. Z. Yao, Queens University, Kingston, Canada]

K. Arakawa et al., Science 318 (2007) 956; K. Arakawa et al., Philos. Mag. Lett. 91 (2011) 86; Z. Yao et al., Philos. Mag. 90 (2010) 4623

The cascade statistics mystery

Size distribution of defects in tungsten: 0.01dpa,
From room temperature to 800°C

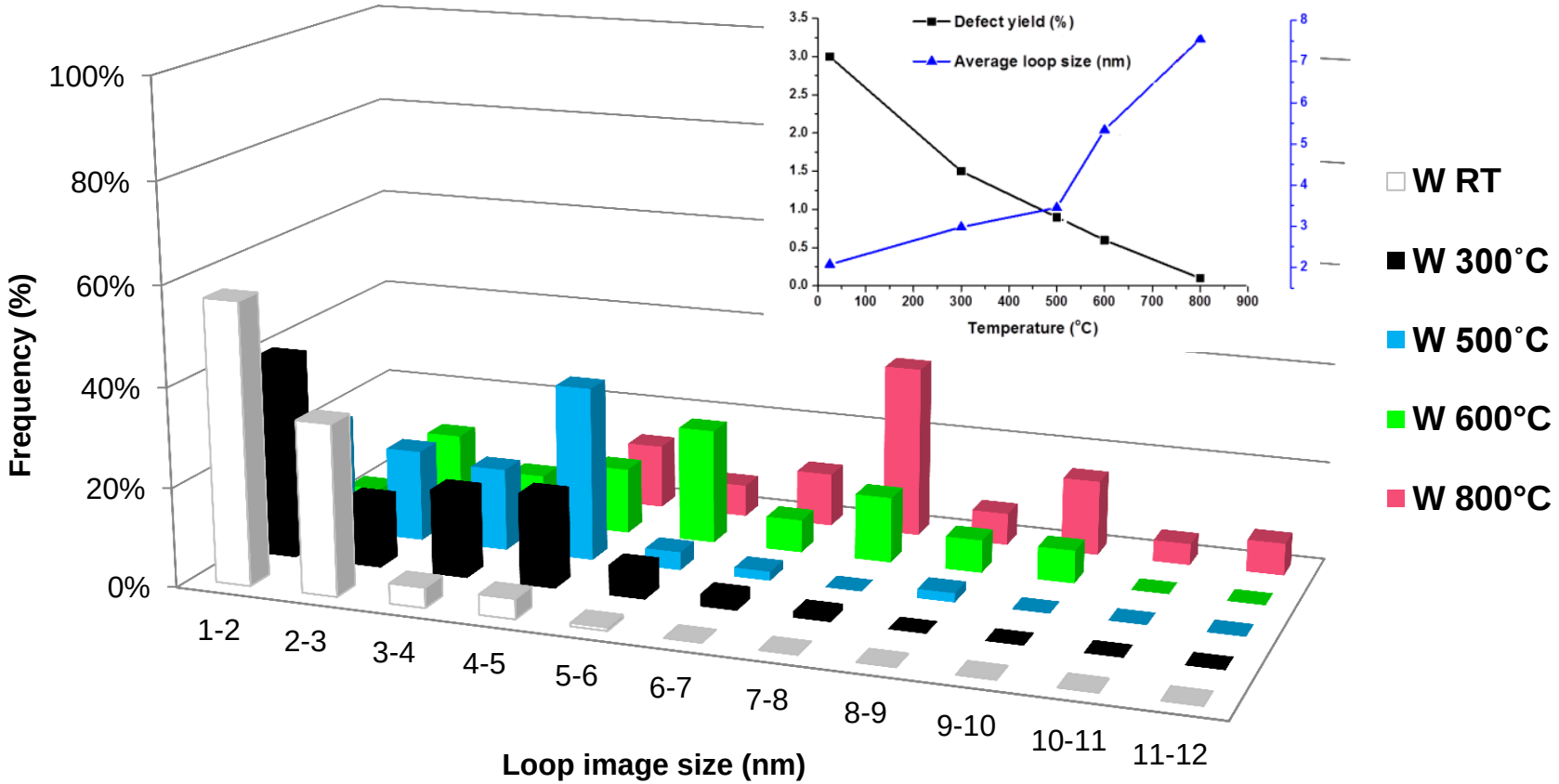

X. Yi, M.A. Kirk *et al.* In situ ion irradiation experiments performed at Argonne National Laboratory in 2012.

United Kingdom Atomic Energy Authority

CCFE is the fusion research arm of the **United Kingdom Atomic Energy Authority**

CCFE CULHAM CENTRE FOR FUSION ENERGY

Inter-defect elastic interaction "potential"

Energy of elastic interaction between two dislocation loops is [Hirth and Lothe, 2nd edition, section 4-5] – this equation assumes that the Burgers vectors of the loops are normal to their habit planes

$$W_{12} = -\frac{\mu}{2\pi}\oint_{C_1}\oint_{C_2}\frac{(\mathbf{b}_1\times\mathbf{b}_2)\cdot(d\mathbf{l}_1\times d\mathbf{l}_2)}{r}$$

$$+\frac{\mu}{4\pi(1-\nu)}\oint_{C_1}\oint_{C_2}(\mathbf{b}_1\times d\mathbf{l}_1)\overleftrightarrow{\mathbf{T}}(\mathbf{b}_2\times d\mathbf{l}_2)$$

Alternatively, if the distance between the defects is greater than their diameter, one can use the dipole approximation, expressing the energy of elastic interaction in terms of defect dipole tensors and the elastic Green's function

$$W_{12} = P_{ij}^a P_{kl}^b \frac{\partial}{\partial R_j}\frac{\partial}{\partial R_l}G_{ik}(\mathbf{R})$$

S.L. Dudarev et al., Phys. Rev. B**81** (2010) 224107; Journ. Nucl. Mater. **455** (2014) 16

Inter-defect elastic interaction "potential"

Elastic Green's function:

$$G_{ik}(R) = \frac{1}{8\pi\mu}\left(\frac{2\delta_{ik}}{R} - \frac{1}{2(1-\nu)}\left[\frac{\delta_{ij}}{R} - \frac{x_i x_k}{R^3}\right]\right)$$

Elastic dipole tensor of a dislocation loop:

$$P_{ij} = \mu\left[\left(b_i A_j + A_i b_j\right) + \delta_{ij}\left(\mathbf{b}\cdot\mathbf{A}\right)\frac{2\nu}{1-2\nu}\right]$$

Relaxation volume of a dislocation loop:

$$\Omega_{rel} = \frac{1}{2\mu}\frac{(1-2\nu)}{(1+\nu)}\mathrm{Tr}P_{ij} = \left(\mathbf{b}\cdot\mathbf{A}\right)$$

Inter-defect elastic interaction "potential"

Dipole (far-field) approximation for the energy of elastic interaction between prismatic dislocation loops.

$$W_{12} = \frac{\mu(b_1A_1)(b_2A_2)}{2\pi}\left\{3\frac{\left[(\mathbf{n}_1\times\mathbf{n}_2)\cdot\mathbf{R}\right]^2}{R^5} - \frac{(\mathbf{n}_1\times\mathbf{n}_2)^2}{R^3}\right\}$$

$$-\frac{\mu(b_1A_1)(b_2A_2)}{4\pi(1-\nu)}\left\{\frac{3}{R^3} - 2\frac{(\mathbf{n}_1\cdot\mathbf{n}_2)^2}{R^3} - 3\frac{(\mathbf{R}\cdot\mathbf{n}_1)^2}{R^5} - 3\frac{(\mathbf{R}\cdot\mathbf{n}_2)^2}{R^5}\right\}$$

$$+\frac{\mu(b_1A_1)(b_2A_2)}{4\pi(1-\nu)}\left\{\frac{15(\mathbf{R}\cdot\mathbf{n}_1)^2(\mathbf{R}\cdot\mathbf{n}_2)^2}{R^7} - \frac{12(\mathbf{R}\cdot\mathbf{n}_1)(\mathbf{R}\cdot\mathbf{n}_2)(\mathbf{n}_1\cdot\mathbf{n}_2)}{R^5}\right\}$$

Energy ~ (size)^4

For a loop, the scalar product **b**·**A** (Burgers vector times the loop area) equals the relaxation volume of the loop. In the above formula, Burgers vectors are assumed normal to the loop habit planes.

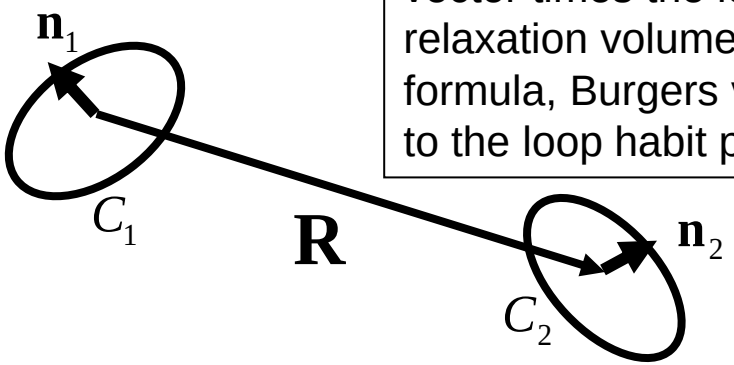

Inter-defect elastic interaction "potential"

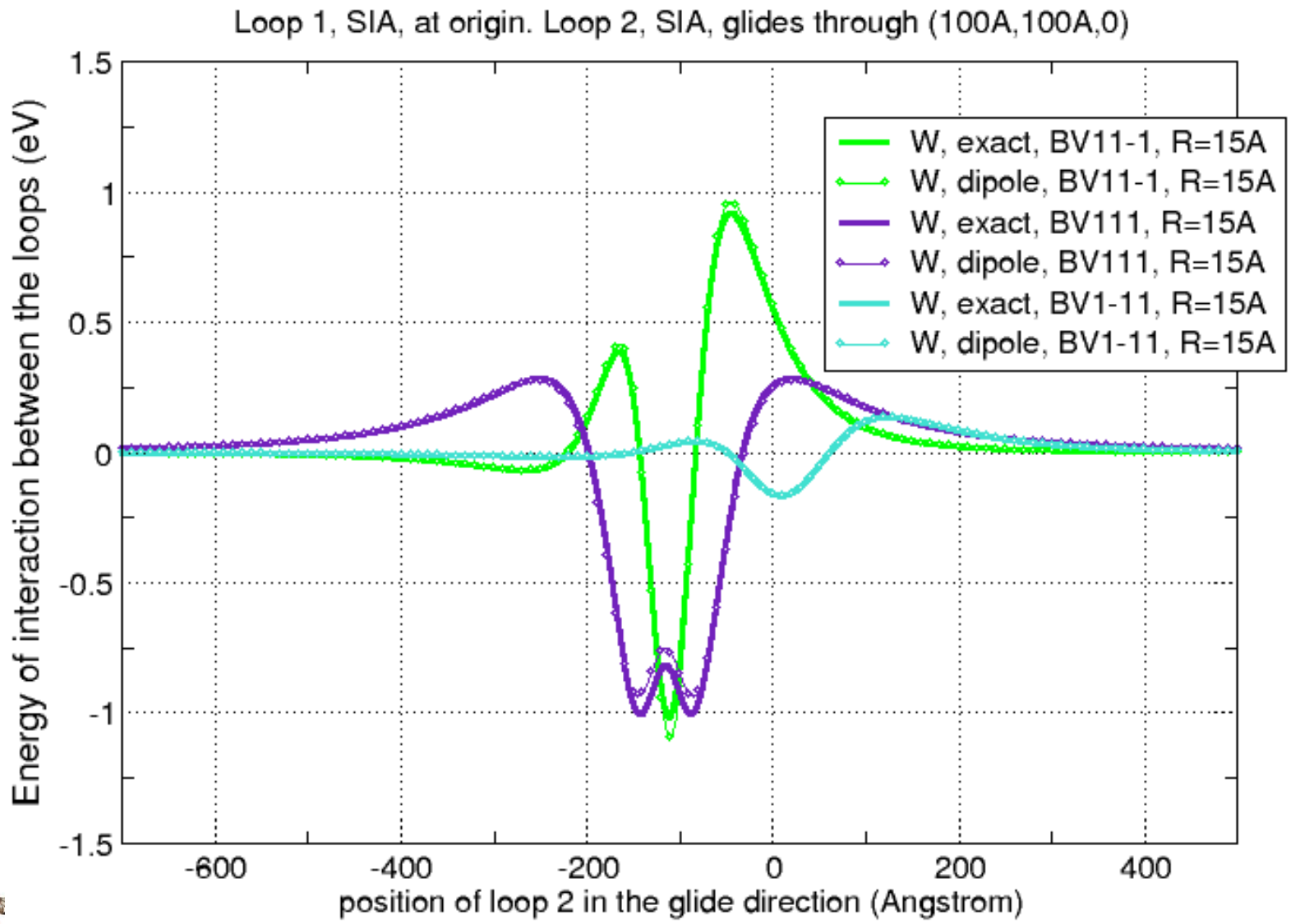

S.L. Dudarev et al., Phys. Rev. B**81** (2010) 224107;
Journ. Nucl. Mater. **455** (2014) 16

Inter-defect elastic interaction “potential”

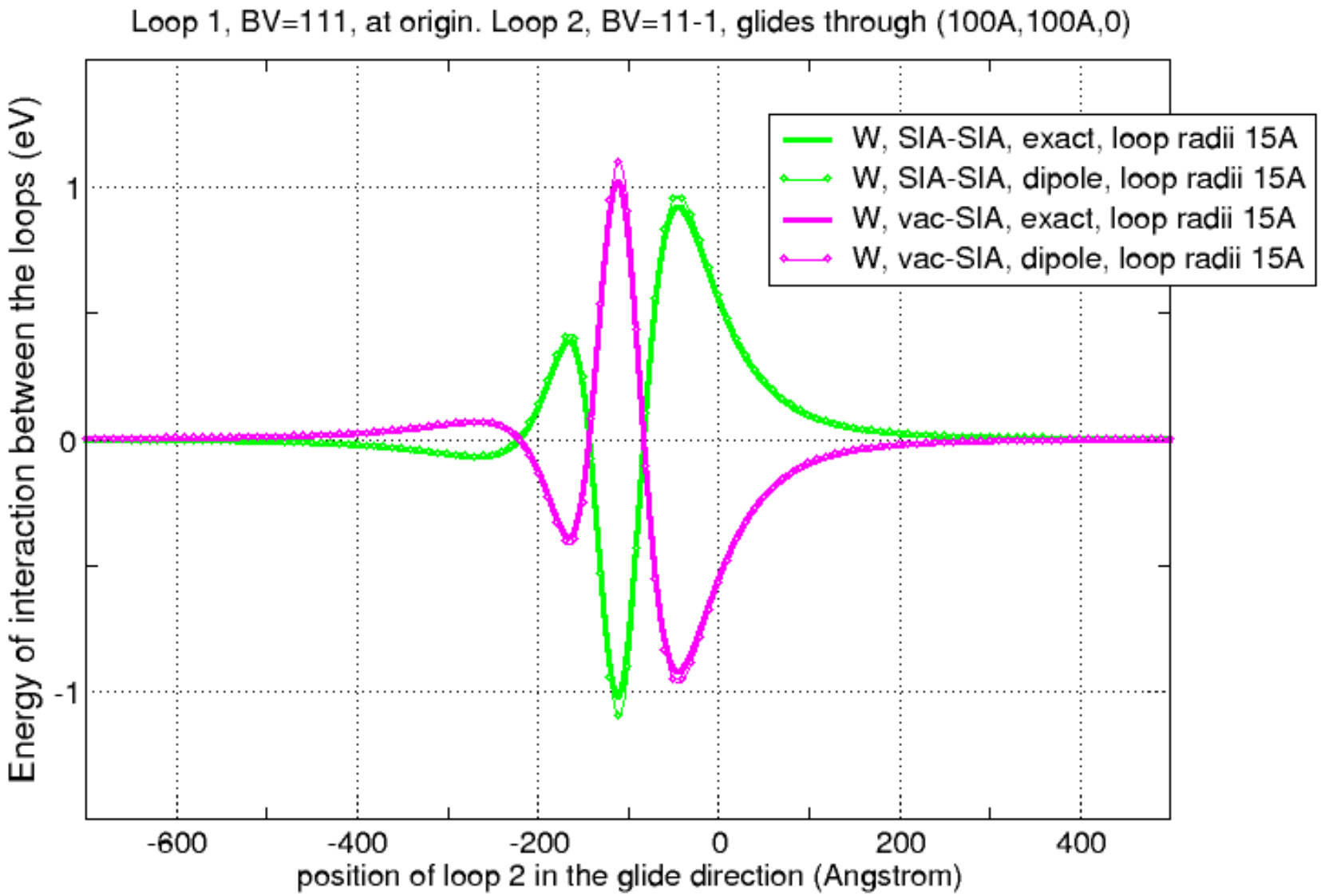

Inter-defect elastic interaction “potential”

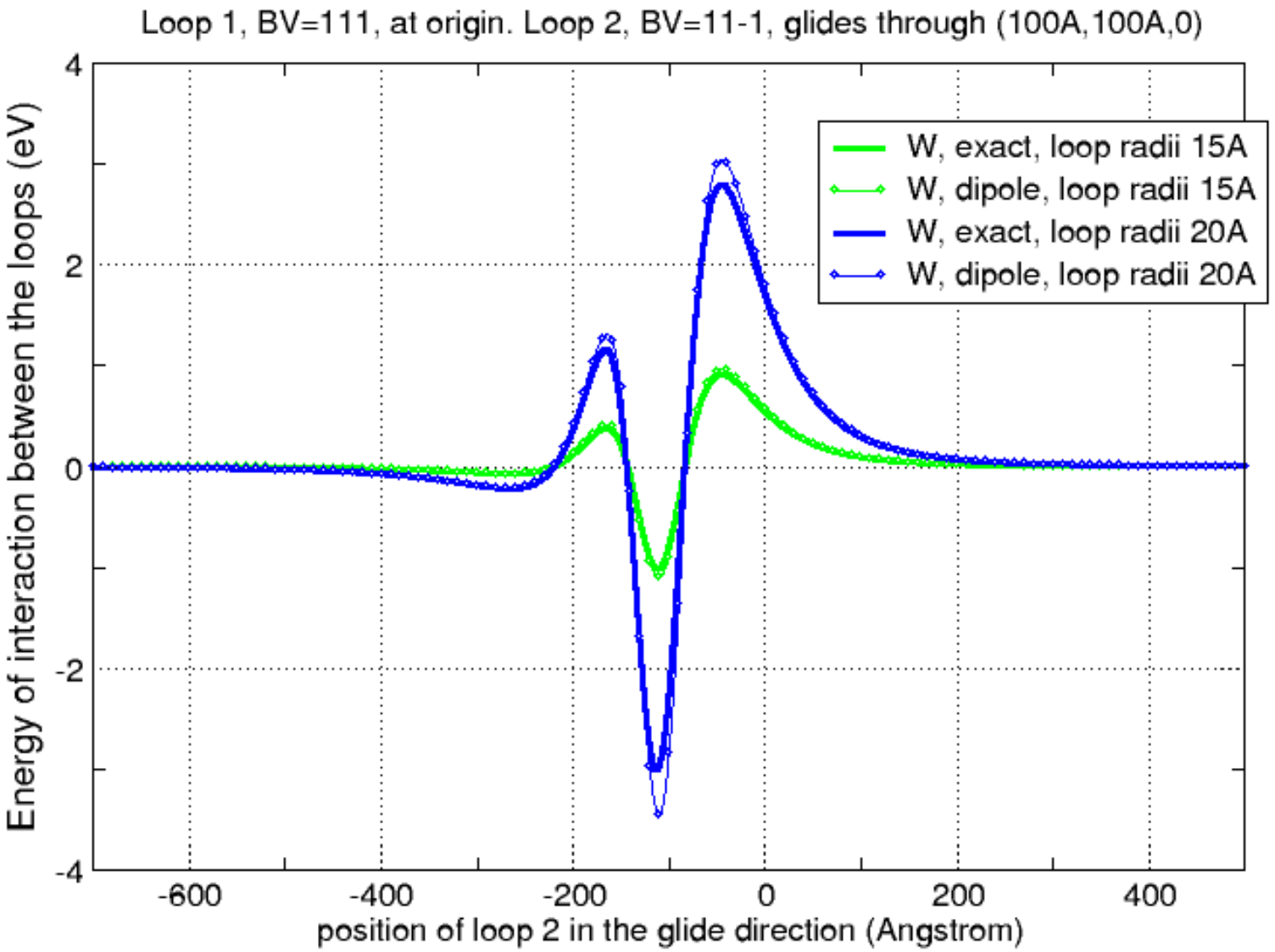

Inter-defect elastic interaction "potential"

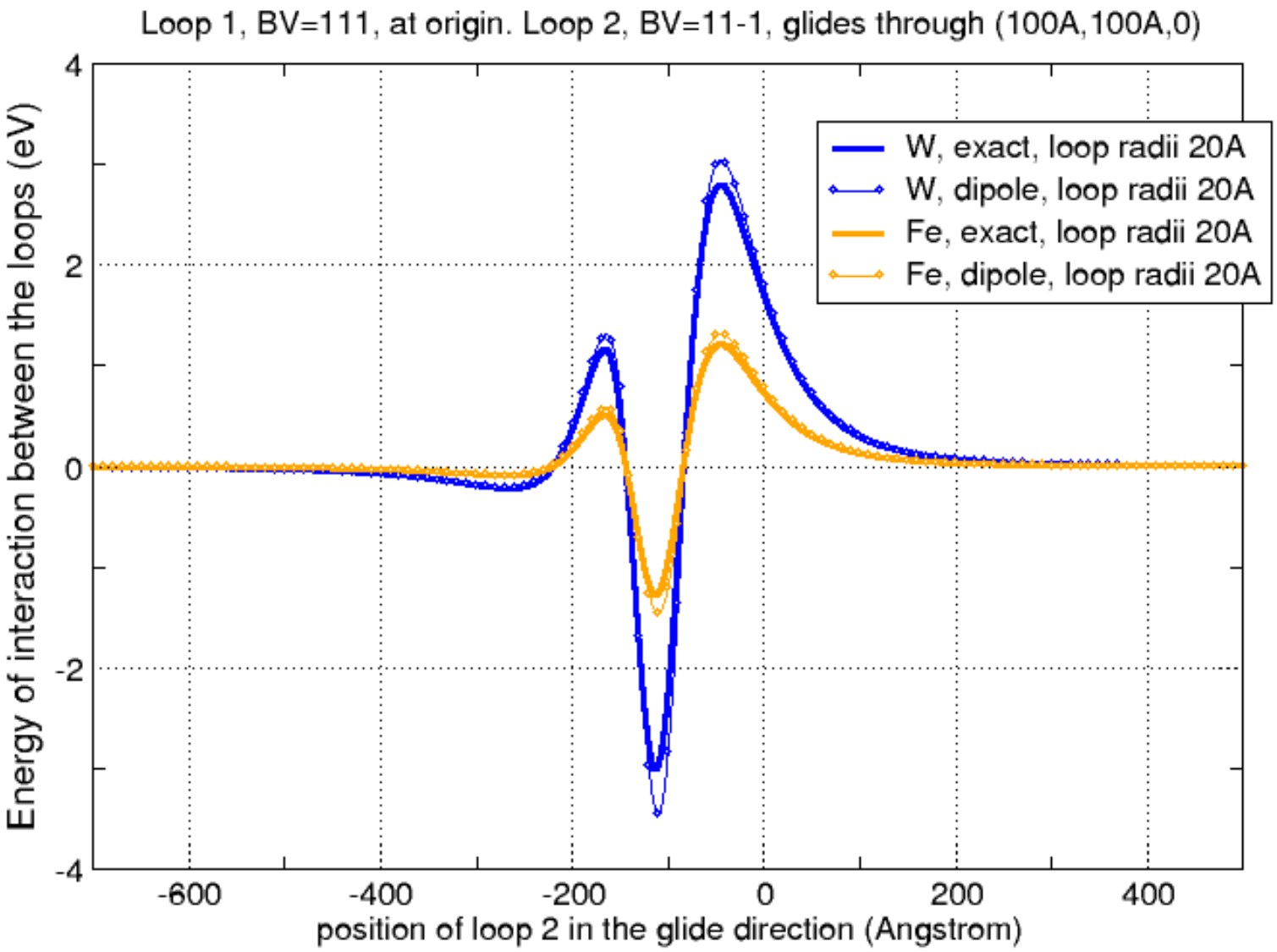

The cascade statistics mystery

Size distribution of defects in tungsten: 0.01dpa,
From room temperature to 800°C

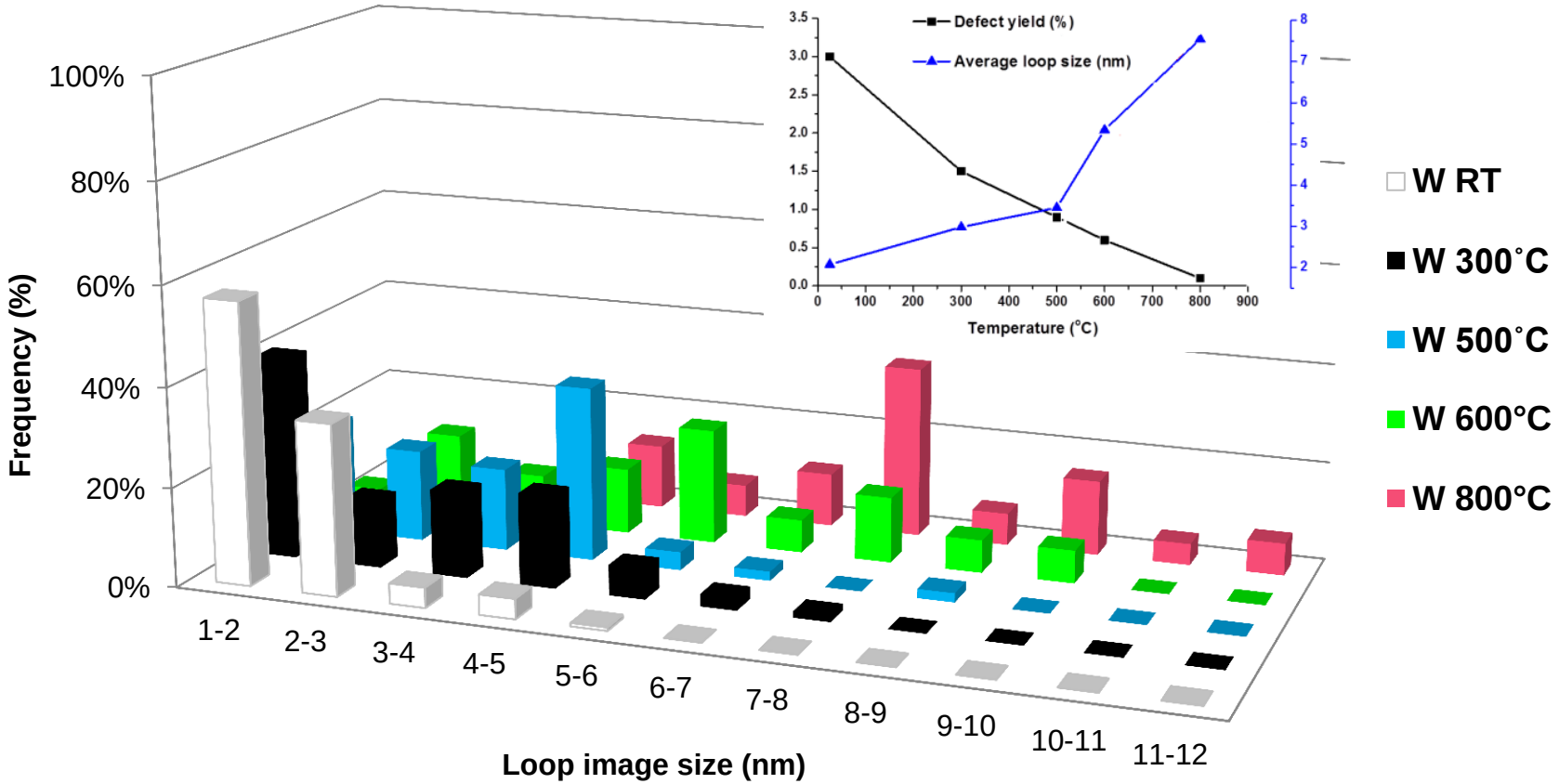

X. Yi, M.A. Kirk *et al.* In situ ion irradiation experiments performed at Argonne National Laboratory in 2012.

United Kingdom Atomic Energy Authority

CCFE is the fusion research arm of the **United Kingdom Atomic Energy Authority**

CCFE CULHAM CENTRE FOR FUSION ENERGY

Comparison to experiment: loop sizes

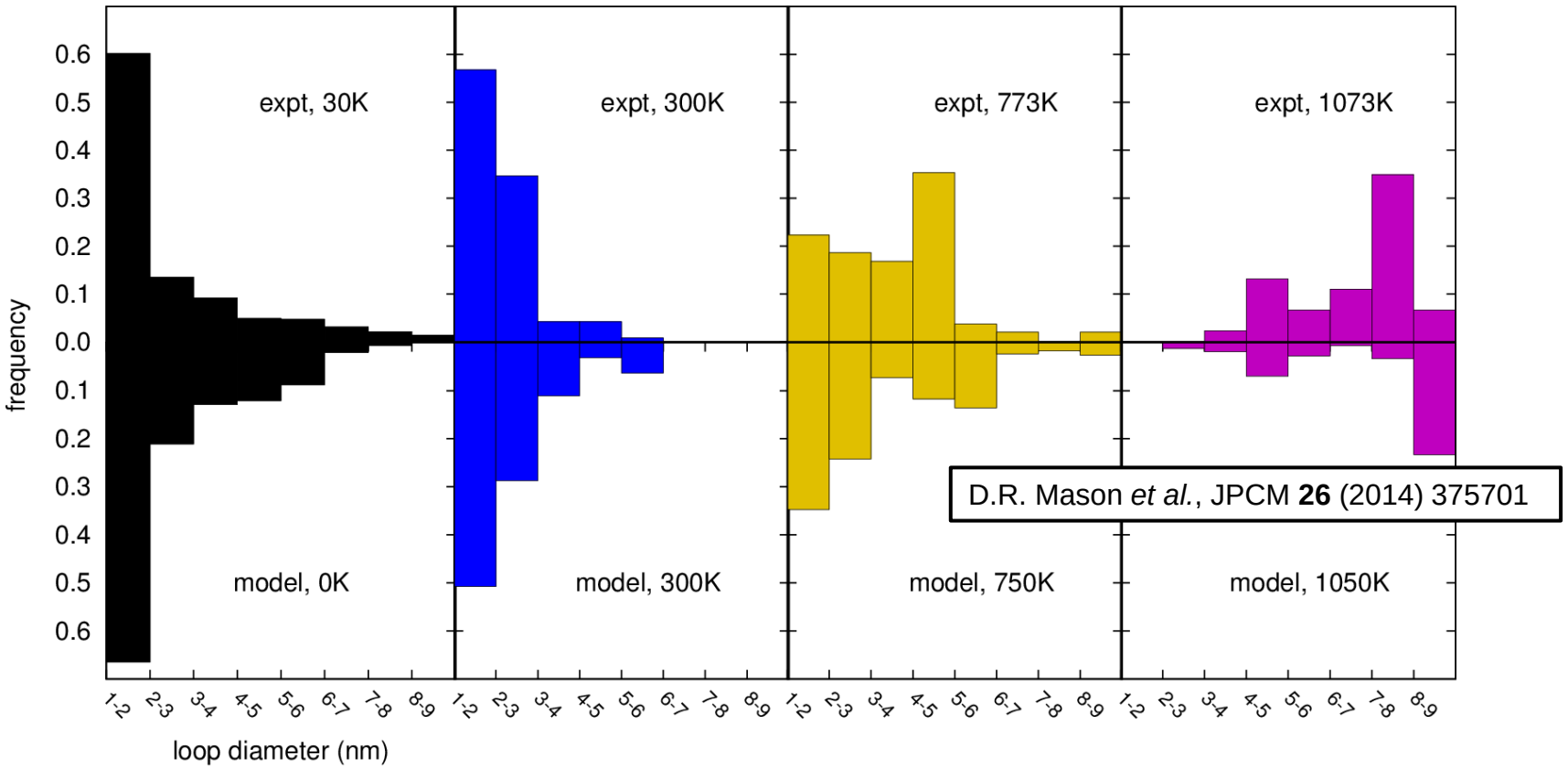

Experimental observation of cascade evolution can be explained by one single hypothesis: interaction between the defects. At higher temperatures: fewer but larger defects. Using the correct cascade statistics of defect sizes is critical.

Evolution of ensembles of interacting dislocation loops

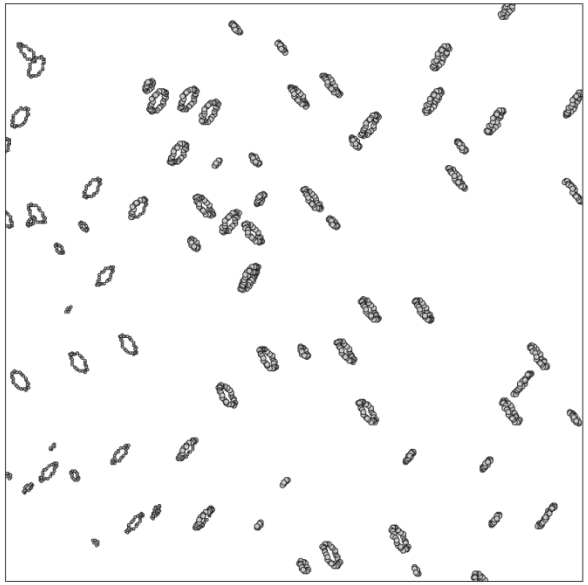

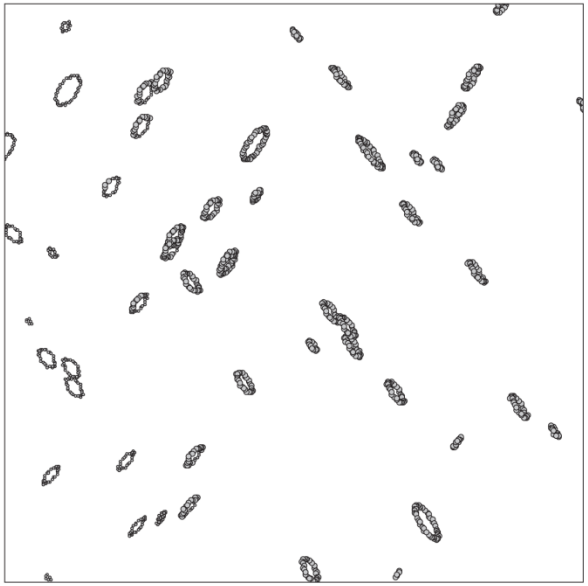

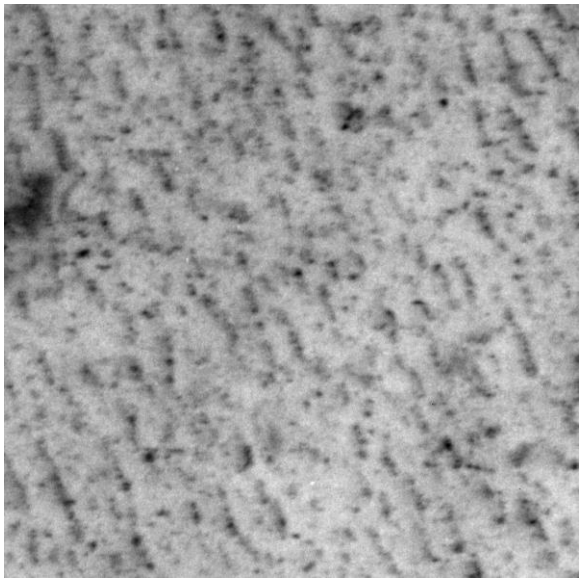

Langevin dynamics: dense ensembles of radiation defects self-order. Elastic interaction between defects. Elastic dipole approximation is accurate in most cases. At short distances dislocation dynamics rules can be applied.

United Kingdom Atomic Energy Authority

S.L. Dudarev et al., Phys. Rev. B**81** (2010) 224107;
Journ. Nucl. Mater. **455** (2014) 16

CCFE is the fusion research arm of the **United Kingdom Atomic Energy Authority**

CCFE CULHAM CENTRE FOR FUSION ENERGY

Macroscopic effects produced by irradiation: lattice swelling

Lattice swelling of helium-implanted tungsten

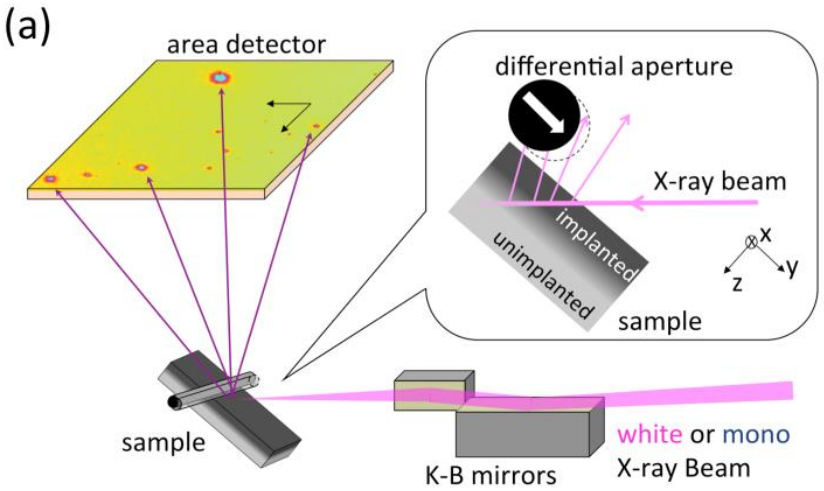

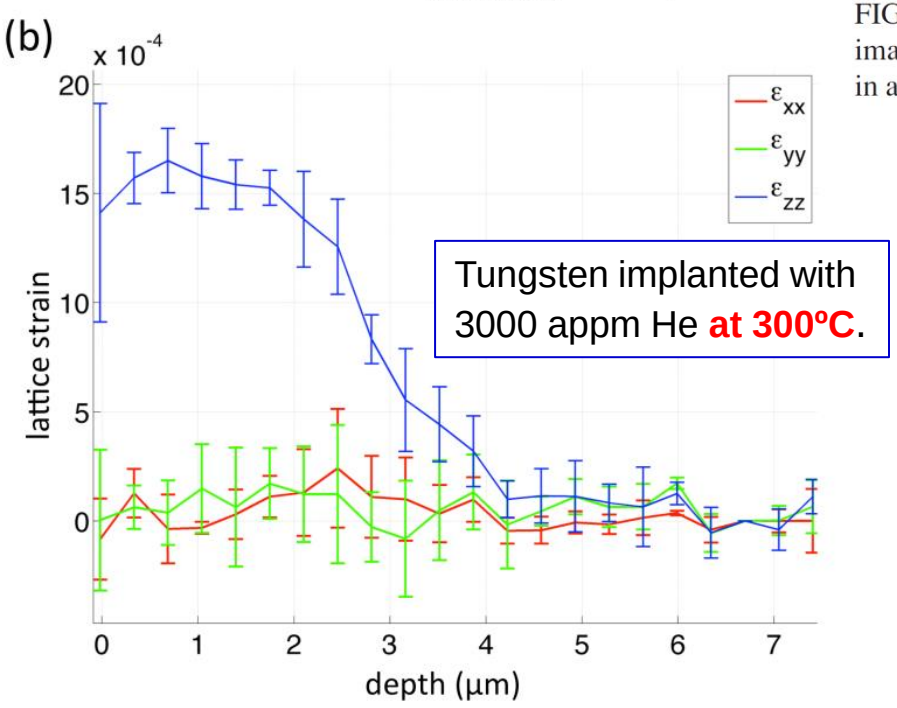

Tungsten implanted with 3000 appm He **at 300ºC**.

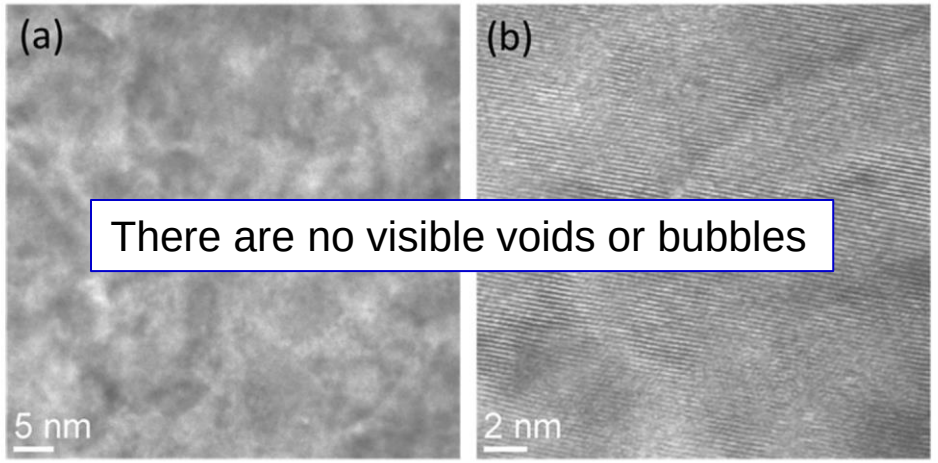

There are no visible voids or bubbles

FIG. 4. TEM micrographs of the 3000 appm He implanted pure W. The image was recorded at ~1 μm underfocus. No Fresnel contrast was observed in a through-focus series indicating no He bubbles are present.

There are two modes of swelling:

1. volume increase associated with the formation of voids in the bulk of the material and “redeposition”of atoms on the surface

2. deformation of the lattice due to local microscopic distortions associated with fine distribution of defects in the lattice.

F. Hofmann et al., Acta Materialia 89 (2015) 352–363

Formation and migration energies of defects (eV)

vacancies	Al	Cu	Au	Ni	Pd	Pt	Pu
E_f	0.580[i]	1.04[d]	0.782[i]	1.37,[e] 1.43,[r] 1.65[r]	1.70[j]	1.18[j]	1.31, 1.36, 1.08[t]
E_m	0.57[m]	0.72[d]	–	1.285,[e] 1.08[r]	–	1.51[j]	–
	V	**Nb**	**Ta**	**Cr**	**Mo**	**W**	**Fe**
E_f	2.51[l]	2.99[l]	3.14[l]	2.64[l]	2.96,[j] 2.96[l]	3.56[l]	2.02,[b] 2.07,[k] 2.15[l]
E_m	0.62[l]	0.91[l]	1.48[l]	0.91[l]	1.28[l]	1.78[l]	0.65,[b] 0.67,[k] 0.64[l]
	C	**Si**	**Ge**	**Be**	**Ti**	**Zr**	**Hf**
E_f	8.2[f]	3.17,[c] 3.29[g]	2.3[h]	0.81,[n] 1.09[o]	1.97,[p] 2.13[q]	2.17,[q] 1.86[s]	2.22[q]
E_m	1.[f]						0.79B, 0.91NB[q]

DFT calculations provide accurate data on the formation and migration energies of defects, but this has no relation to swelling!

SIA	⟨111⟩	⟨110⟩	⟨100⟩	Tetrahedral	Octahedral	E_m
Fe	4.66,[b] 4.45[c]	3.94,[b] 3.75[c]	5.04,[b] 4.75[c]	4.26[c]	4.94[c]	0.34[c]
V	3.37,[d] 3.14[e]	3.65,[d] 3.48[e]	3.92,[d] 3.57[e]	3.84,[d] 3.69[e]	3.96,[d] 3.62[e]	
Nb	5.25[d]	5.60[d]	5.95[d]	5.76[d]	6.06[d]	
Ta	5.83[d]	6.38[d]	7.00[d]	6.77[d]	7.10[d]	
Cr	5.66[d]	5.68[d]	6.64[d]	6.19[d]	6.72[d]	
Mo	7.42,[d] 7.34[e]	7.58,[d] 7.51[e]	9.00,[d] 8.77[e]	8.40,[d] 8.20[e]	9.07,[d] 8.86[e]	
W	9.55[d]	9.84[d]	11.49[d]	11.05[d]	11.68[d]	~0.013
Al	1.959[f]	1.869[f]	1.579[f]	1.790[f]	1.978[f]	0.084[f]
Ni	4.69[g]	4.99[g]	4.07[g]	4.69[g]	4.25[g]	0.14[g]
Si	3.84[h]	3.80 (hexagonal)	3.85 (caged)	4.07[h]	4.8	0.18[h]

Annual Review of Materials Research **43** (2013) 35-61

Statistical elasticity theory of defect-induced swelling

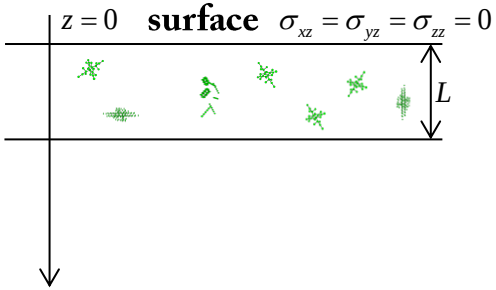

Each defect produces its own field of elastic displacements:

$$u_i(\mathbf{r}) = -P_{ks}^{(\alpha)} \frac{\partial}{\partial x_s} G_{ik}(\mathbf{r} - \mathbf{R}_\alpha)$$

$P_{ks}^{(\alpha)}$ - defect dipole tensor.

$$G_{ik}(R) = \frac{1}{8\pi\mu}\left(\frac{2\delta_{ik}}{R} - \frac{1}{2(1-\nu)}\left[\frac{\delta_{ij}}{R} - \frac{x_i x_k}{R^3}\right]\right)$$

Calculation of the stress tensor: the density of forces exerted by the defects on the surrounding material:

$$F_i(\mathbf{r}) = -\sum_\alpha P_{il}^{(\alpha)} \frac{\partial}{\partial x_l} \delta(\mathbf{r} - \mathbf{R}_\alpha)$$

$$\frac{\partial}{\partial x_k}\sigma_{ik} + F_i(\mathbf{r}) = 0$$

The stress tensor is related to the strain tensor through the Hooke's law equation

$$\sigma_{ij} = \frac{E}{1+\sigma}\left(u_{ij} + \frac{\sigma}{1-2\sigma}u_{ll}\delta_{ij}\right)$$

United Kingdom Atomic Energy Authority

F. Hofmann et al., Acta Materialia 89 (2015) 352–363

CCFE CULHAM CENTRE FOR FUSION ENERGY

Statistical elasticity theory of defect-induced swelling

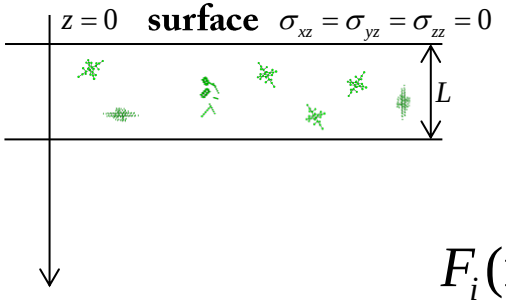

We are interested in stresses averaged over the positions of defects in the implanted layer:

$$F_i(\mathbf{r}) = -\sum_\alpha P_{il}^{(\alpha)} \frac{\partial}{\partial x_l} \int_V \frac{dR_\alpha}{V} \delta(\mathbf{r}-\mathbf{R}_\alpha) = -\frac{1}{V}\sum_\alpha P_{il}^{(\alpha)} \frac{\partial}{\partial x_l}\Theta(\mathbf{r})$$

Function $\Theta(\mathbf{r})$ equals 1 inside the implanted layer, and it is zero outside the layer. In practice $\Theta(\mathbf{r}) = \Theta(z)$ where $\Theta(z) = 1$ for 0<z<L.

$$F_z(z) = -\sum_A n^{(A)} P_{zz}^{(A)} \frac{\partial}{\partial z}\Theta(z) = \sum_A n^{(A)} P_{zz}^{(A)} \left[\delta(z-L) - \delta(z)\right]$$

The above equation provides a starting point for the analysis below:

$$\frac{\partial}{\partial z}\sigma_{zz} + F_z(z) = 0; \qquad \frac{\partial}{\partial z}\sigma_{xz} = \frac{\partial}{\partial z}\sigma_{yz} = 0$$

Boundary conditions at the surface: $\sigma_{xz}(z=-0) = \sigma_{yz}(z=-0) = \sigma_{zz}(z=-0) = 0$

Statistical elasticity theory of defect-induced swelling

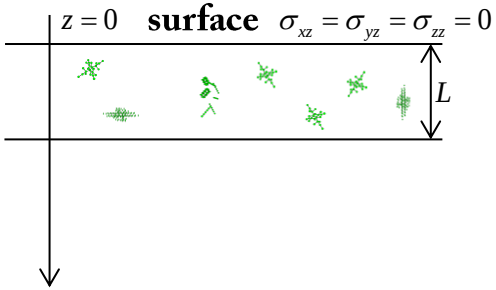

A very important equation relating the defect dipole tensor and the relaxation volume of the defect:

$$\mathrm{Tr}P_{il}^{(A)} = \frac{E}{1-2\sigma}\Omega_{rel}^{(A)}$$

Stresses and strains from elasticity:

$$\frac{\partial}{\partial z}\sigma_{zz} = \frac{1}{3}\sum_A n^{(A)}\mathrm{Tr}\left(P_{ij}^{(A)}\right)\left(\delta(z)-\delta(z-L)\right),$$

$$\sigma_{zz} = \frac{1}{3}\sum_A n^{(A)}\mathrm{Tr}\left(P_{ij}^{(A)}\right)\left(\Theta(z)-\Theta(z-L)\right)$$

$$u_{zz} = \frac{(1+\nu)(1-2\nu)}{E(1-\nu)}\sigma_{zz}$$

Swelling:

$$u_{zz} = \frac{(1+\nu)}{3(1-\nu)}\sum_A n^{(A)}\Omega_{rel}^{(A)}\left(\Theta(z)-\Theta(z-L)\right)$$

Swelling is proportional to the sum of products of defect concentrations and defect relaxation volumes.

F. Hofmann et al., Acta Materialia 89 (2015) 352–363

Statistical elasticity theory of defect-induced swelling

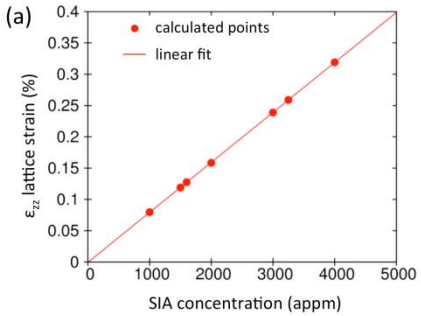

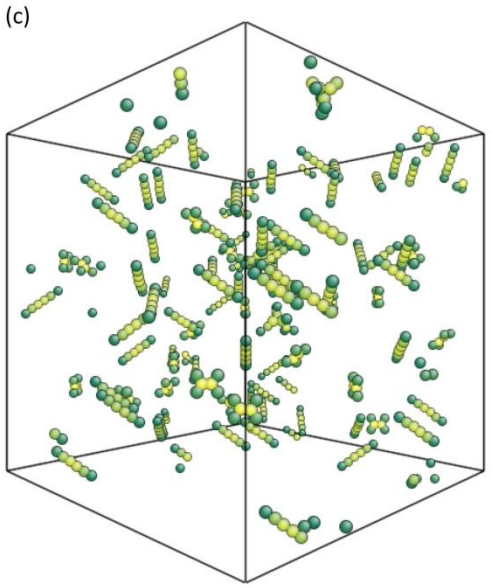

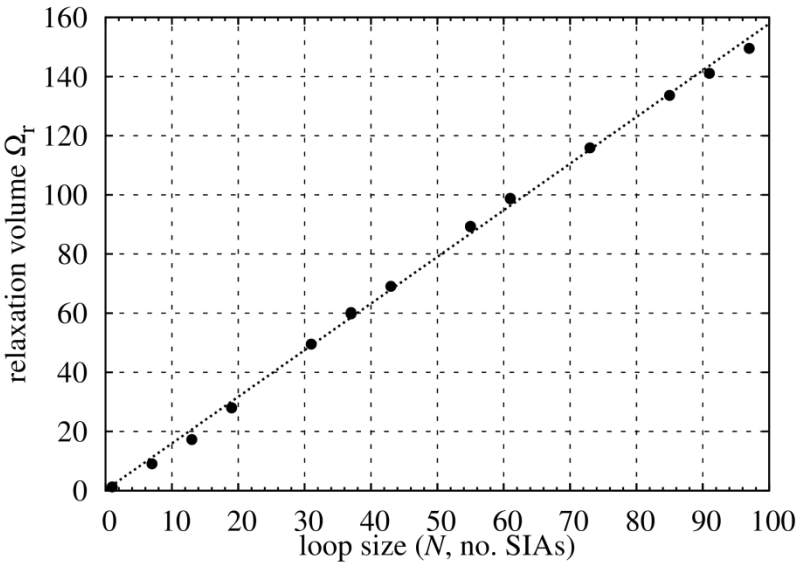

Table 1. Relaxation volumes, Ω_r, of various defects in pure tungsten. Values are calculated by DFT and are given in atomic volume units Ω_0. (a) Relaxation volumes of vacancies and self-interstitials (V: vacancy, V_2: di-vacancy, V_3: tri-vacancy, SIA: self-interstitial atom). (b) Relaxation volumes of interstitial He_n clusters. (c) Relaxation volumes of He_nV clusters.

(a) Relaxation volumes of vacancies and self-interstitial atom defects

V	V_2 (1NN)	V_2 (2NN)	V_2 (3NN)	V_3 (1NN(2) + 2NN)	<111> SIA
−0.37 −0.34[60] −0.38 [61]	−0.72 −0.65 [60]	−0.79 −0.74 [60]	−0.76 −0.69 [60]	−1.08	1.68

(b) Relaxation volumes of interstitial helium clusters

He (tetra)	He (octa)	He_2 (tetra)	He_3 (tetra)	He_4 (tetra)	He_5 (tetra)
0.36 0.33 [62]	0.37 0.34 [62]	0.80	1.16	1.65	2.03

(c) Relaxation volumes of helium – vacancy clusters

HeV (tetra)	HeV(octa)	He_2V (tetra)	He_3V (tetra)	He_4V (tetra)	He_5V (tetra)	He_6V (tetra)
−0.24	−0.23	−0.06	0.14	0.38	0.71	1.09

F. Hofmann et al., Acta Materialia 89 (2015) 352–363

Statistical elasticity theory of defect-induced swelling

Final analysis and conclusions

- Helium has strong affinity to vacancies, leading to the formation of helium-vacancy complexes. Self-interstitial atoms remain in the bulk, and may cluster (this is not critical, since clustering does not have a strong effect on the relaxation volume per defect, see previous slide)

- If we assume that helium is in He-V complexes then ~3100 appm He-V and 3100 appm self-interstitial atoms, resulting in swelling $u_{zz} = 2650 \cdot 10^{-6}$. This is approximately twice the experimentally observed value.

- If we assume that helium is in He_2-V complexes, then ~1550 appm He_2-V and 1550 appm self-interstitial atoms results in swelling $u_{zz} = 1500 \cdot 10^{-6}$. This is almost exactly what I observed experimentally.

- Swelling – in this particular experiment, where He was implanted at a relatively low temperature of 300ºC, results almost entirely from the accumulation of self-interstitial atom defects (which may or may not cluster). Helium-vacancy defects have smaller relaxation volumes and do not contribute significantly to swelling.

Radiation damage effects in tungsten

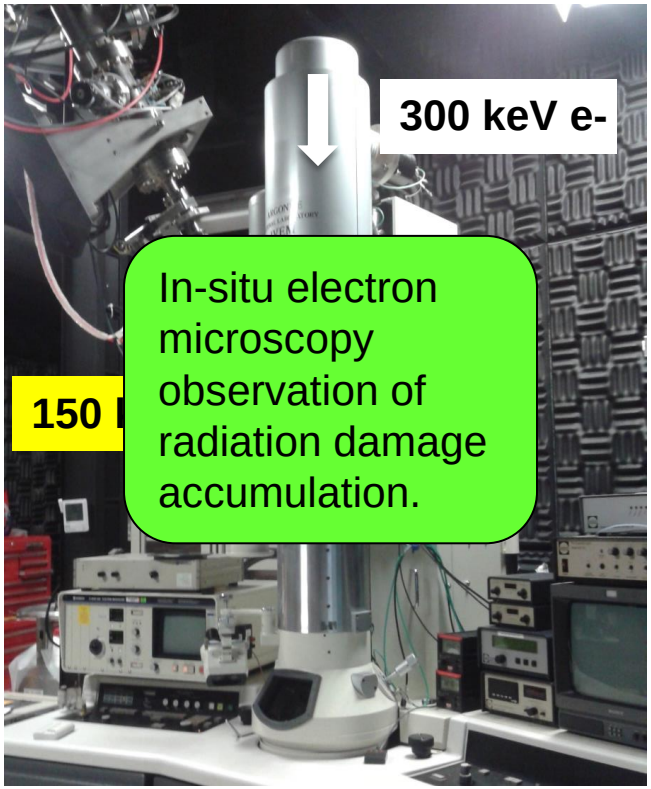

In-situ electron microscopy observation of radiation damage accumulation.

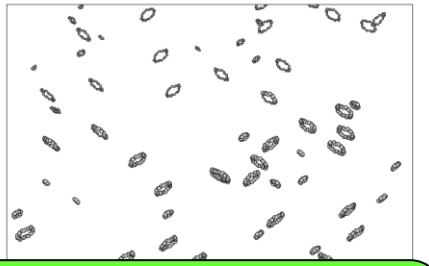

Ordering of radiation defects in irradiated tungsten.

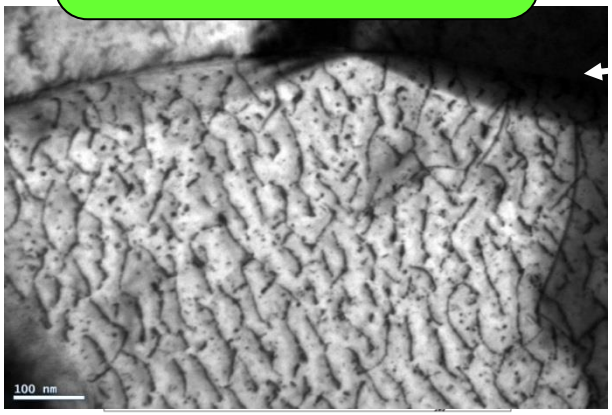

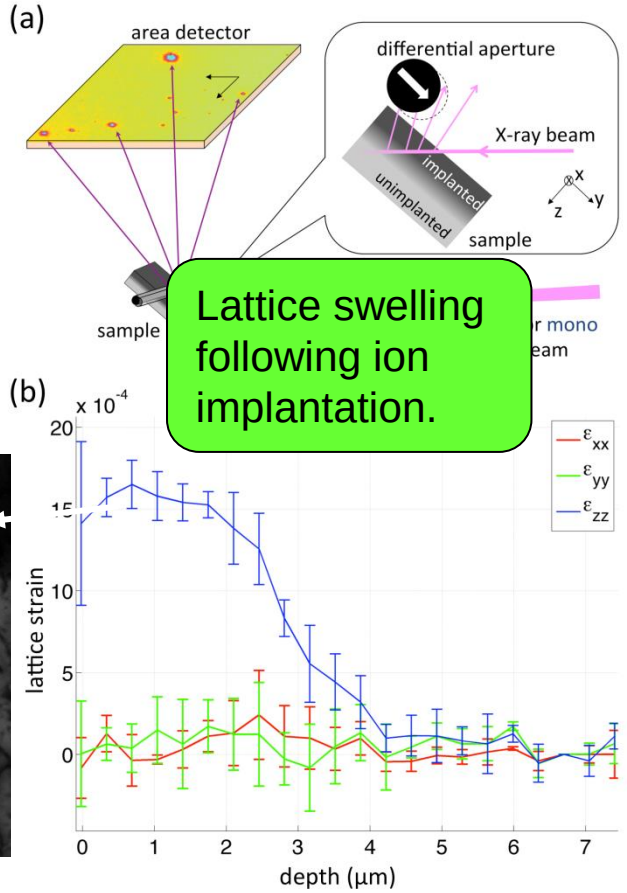

Lattice swelling following ion implantation.

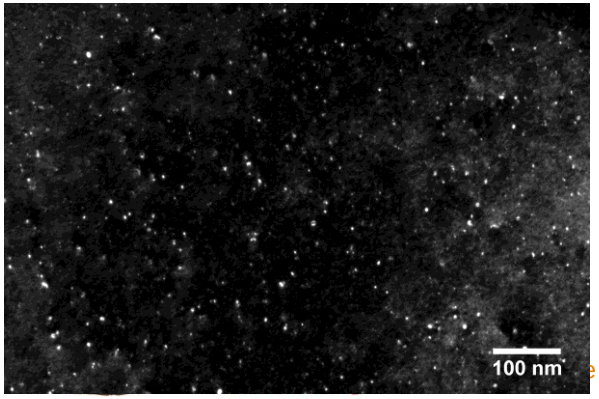

Left: X. Yi, A.E. Sand, D.R. Mason, M.A. Kirk, S.G. Roberts, K. Nordlund, and S.L. Dudarev, EuroPhysics Letters (EPL) **110** (2015) 36001

Centre: S.L. Dudarev, K. Arakawa, X. Yi, Z. Yao, M.L. Jenkins, M.R. Gilbert, P.M. Derlet, Journal of Nuclear Materials 455 (2014) 16–20

Right: F. Hofmann, D. Nguyen-Manh, M.R. Gilbert, C.E. Beck, J.K. Eliason, A.A. Maznev, W. Liu, D.E.J. Armstrong, K.A. Nelson, and S.L. Dudarev, Acta Materialia **89** (2015) 352–363

CENTRE FOR FUSION ENERGY